Blockchain Operations in the Presence of Security Concerns

(Authors' names blinded for peer review)

Problem Definition: A blockchain system, such as Bitcoin or Ethereum, validates electronic transactions and stores them in a chain of blocks without a central authority. *Miners* with computing power compete for the right to create blocks according to a pre-set protocol and in return earn fees paid by *users* who submit transactions. Due to security concerns caused by *decentralization*, a transaction is confirmed after a number of additional blocks are subsequently extended to the block containing it, which introduces intricate interplay between miners and users. This paper studies the system equilibrium and optimal design of a blockchain. **Methodology/results:** Such a system essentially operates as a single server queue with batch services based on a fee-based priority discipline, albeit with distinctive features due to the security concerns. We analyze how miners' participation decisions interact with users' participation and fee decisions in equilibrium, and identify an optimal design when the goal is to maximize total throughput or users' utility. We validate our model and analytical results using data from Bitcoin. **Managerial implications:** Our analyses reveal that miners and users may end up in either a vicious or virtuous cycle, depending on the initial system state. Under both objectives, an optimal system (may not be the unique one) runs at its full capacity and a block size as small as possible, which confirms a current trend in practice, and non-zero entrance fees in general.

Key words: Service Operations; Queueing Theory; Game Theory.

1. Introduction

In the past decade, *cryptocurrencies*, or digital assets that function as a means of exchange enabled by the blockchain technology, have exploded as a significant global phenomenon. While Bitcoin and Ethereum are the most commonly known, there are more than five thousand cryptocurrencies in the global market with a daily trading volume exceeding \$60 billion (https://www.coinmarketcap.com). Furthermore, according to https://www.statista.com, the market capitalization of these cryptocurrencies is close to \$2 trillion, representing a hundred-fold increase since 2015, and the estimated number of unique active users has grown from between $0.3 \sim 1.3$ million in 2013 to over 74 million by June 2021. Furthermore, these cryptocurrencies have generated an entire financial ecosystem comprising exchanges, financial derivatives, and mining businesses, making them viable investment assets. For example, Bitcoin had generated over \$63 million in mining revenue per day in June 2021, not to mention the additional revenue generated from the sales of mining hardware and the provision of cloud mining and remote hosting services as well as price appreciation gains.

Cryptocurrencies have also led to the development of sizable new business platforms and new forms of peer-to-peer economic activities.

These economic activities differ from traditional *centralized* payment systems which are processed through a single trusted central agency. For instance, fiat cash is issued by central banks that possess reliable anti-counterfeiting technology while credit cards and digital payment services are provided by trusted financial institutions. In contrast, cryptocurrencies are based on a *decentralized* participant-level exchange following a pre-specified protocol. Since these exchanges are not conducted under the auspices of a credible agency, they are open to potential adversarial attacks and thus the underlying protocol must be able to ensure consensus in the presence of such an adversary. One protocol that has been established to ensure consensus is *proof-of-work* (PoW). PoW is the most popular consensus mechanism and supports several mainstream cryptocurrencies such as Bitcoin and Ethereum, representing over two-thirds of the cryptocurrency market. In our paper, we examine blockchain operations under the PoW protocol.

Under a proof-of-work mechanism, users submit transactions to a public buffer called a *mempool.* These transactions then await processing by miners, who process the transactions in batches according to the following procedure. At any time, each miner selects a number of transactions from the mempool not exceeding a pre-specified upper limit (1 megabyte for Bitcoin). Each miner then packages the selected transactions into a block and identifies an existing block on the blockchain as the new block's predecessor. To append the new block to its predecessor, the miner needs to solve a cryptographic puzzle before other miners do, which is also referred to as mining or hashing a block. Solving the puzzle requires a specifically designed computing machine such as GPU or ASIC and considerable computing power (Antonopoulos 2014). In this system, miners essentially engage in a competition to earn the right for a miner's block to be accepted by other miners, as once a block is created, all its transactions are considered to be processed and hence are removed from the mempool. Given the computing power required to compete in arriving at the solution, miners equipped with more computing power have a greater chance of winning the competition.

Note that this process of appending a new block to an existing one leads to a *tree* of blocks. Blocks that are carried on the longest chain indicate the most extensive proof-of-work and are included in a public ledger. They are also an indication of honest miner activity, as opposed to blocks not carried on the longest chain, which reflect malicious work done by adversaries. Thus, we refer to miners who append their blocks to the end of the longest chain as *honest* ones and those who don't as *adversaries.* Since the decentralized nature of the process creates the possibility of adversaries, blocks within the longest chain are considered confirmed only after a certain number of blocks are attached to them, referred to as the *confirmation latency*. This confirmation latency provides a means of preventing adversary activity, as it would take a disproportionally large amount of computing power for an adversary to fork a branch fast enough to overrun the honest chain and invalidate a transaction after its confirmation. Hence, as long as the computing power of honest miners exceeds that of adversarial ones, consensus can be established with a high probability. Thus, transaction records contained within the longest chain of blocks form a secure and irrevocable public ledger, as demonstrated by the successful transaction management of various cryptocurrencies.

As indicated, the successful operation of a blockchain system depends on the participation of honest miners, who incur costs in terms of computing power required to compete. Miners receive a *block reward*, or fixed fee, in the form of newly issued coins, in addition to transaction fees associated with all the transactions in the block provided by the users. To prevent inflation and limit the total supply of new coins, mainstream cryptocurrencies have instituted exponentially-diminishing block reward policies. For example, Bitcoin starts with 50 bitcoins as a block reward and halves the amount every $210,000$ blocks or roughly every four years according to the block production speed. Eventually, block rewards will completely disappear, leaving miners to rely solely on transaction fees as their mining income. Thus, although miners' main source of income is still the block reward which remains relatively stable in four-year intervals in the near future, we focus mainly on the situation where miners have to rely on transaction fees as the block reward is diminishing fast and will eventually disappear.

On the user side, users who need their transactions processed by miners will decide to participate based on transaction queueing time, the transaction fee, and the confirmation latency. To obtain a shorter queueing time, users may need to pay a higher transaction fee to motivate miners to select their transactions over others. The confirmation latency to guarantee a high probability that the system will not be attacked by adversaries relies on the collective computing power of honest miners. The higher computing power honest miners have, the harder it is for adversaries to attack the system and the shorter the confirmation latency is needed.

Thus, a user's participation and fee decisions are affected by the collective ability of honest miners to validate transactions, while a miner's computing power expenditure decision is determined by transaction fees and block rewards, although the latter will disappear eventually. A greater number of users willing to participate and pay higher fees incentivizes honest miners to provide a greater amount of computing power, leading to ultimately a healthier system and shorter confirmation latency. Thus, the interplay between users and miners exhibits an intricate dynamic due to the endogenous security risks of the decentralized system and one which has received little attention in the academic literature. This paper attempts to fill this void in the literature by first building an economic model that captures the unique features of cryptocurrency systems as payment services, and then using this model to analyze participant behavior and the optimal system design.

To do so, we first study the dynamics in the mempool under a homogeneous user utility function to capture users' rational behavior in equilibrium, assuming away the block reward which will disappear in the future. We first note that the process of solving a cryptographic puzzle is essentially a continuous flipping of a coin with an extremely low success probability. Miners solve each puzzle independently and a miner's computing power determines the number of trials he is able to conduct per unit of time. A new block is produced when a puzzle is solved by a miner. Hence, the number of trials needed to mine a block is geometrically distributed with a low success probability from each trial and hence, can be well approximated by an exponential random variable. Once a block is produced, all honest miners proceed to a new puzzle for a new block. Thus, a blockchain system can be viewed as one where all honest miners pool their computing power and work *collectively* as a *single server* with exponential service times. To ensure a stable block production rate, the protocol dynamically adjusts the mining difficulty, i.e., the small success probability, according to the total computing power in the system. Therefore, the block processing rate remains constant even though the honest miners' participation level varies over time. If we assume transactions arrive according to a Poisson process, then the mempool essentially operates as an $M/M/1$ queue with prioritized batch service. While honest miners cannot increase the block production rate, their total computing power can affect the confirmation latency, which in turn impacts users' participation and fee decisions and thus impacts the honest miners' participation decisions. We characterize the equilibrium behavior of both users and miners and delineate the optimal system design using the model. We then verify our model with cryptocurrency data from Bitcoin and discuss our results.

Our study contributes to the existing literature on blockchain systems in several important ways. To the best of our knowledge, it is the first to incorporate the security features of such systems in analyzing the intricate interplay between users and miners, leading to important findings and insights into how a blockchain system works. Specifically, we provide three important insights.

1. Assuming that honest miners' participation is proportional to the level of transaction fees, we show how the equilibrium behavior of the users and miners is interdependent, and how the ultimate health of the system depends on the initial participation of honest mining power from an evolutionary point of view. Thus, our results suggest that it is critical for a blockchain system to attract a sufficient number of honest miners at the beginning.

2. Our findings suggest that the blockchain design to achieve maximal throughput or user welfare, in terms of mining rate, block size, and minimum transaction fee requirement, entails running the system at its full capacity, which contradicts some existing research that recommends holding back capacity in order to generate higher transaction fees. Our results also confirm a current trend in practice that suggests setting a block size as small as possible.
3. We analytically identify user behavior under heterogeneous waiting costs and conduct numerical experiments using real block rewards and transaction fees from Bitcoin. We show that classifying users into multiple types leads to a better fit of user behavior to real data.

The rest of the paper is organized as follows. After a literature review in Section 2, we introduce our detailed model in Section 3 and derive the equilibrium behavior in Section 4. The optimal system parameters are derived in Section 5. We discuss some extensions of our model in Section 6 and conduct a numerical study using real data in Section 7. The paper concludes in Section 8 and all the proofs can be found in the Electronic Companion.

2. Literature Review

Since the inception of Bitcoin, the first blockchain system designed by and documented in Nakamoto (2008), a number of systems have evolved to enable users to establish trust in a decentralized setting. These systems seek to develop alternative mechanisms to achieve the same functionality as Bitcoin with better performance. For instance, Algorand Gilad et al. (2017) use a modification of the Byzantine agreement algorithm by Feldman and Micali (1988) to reach consensus, while Conflux Li et al. (2018) and Prism Bagaria et al. (2018) utilize a graph structure rather than a simple chain structure to store transaction contents. To reach consensus efficiently, Conflux relies on the weights of the graph vertices while Prism incorporates a sortition and group voting mechanism to improve throughput and reduce latency. Blockchain systems have also been extended to applications beyond the processing of transaction payments. For instance, Ethereum implements state machines on a Bitcoin-like system that allows users to sign and fulfill contracts in a decentralized manner (Wood (2014)). Since these blockchain systems are focused on real-world applications, the design reliability issue has only been discussed with informal arguments, e.g., the recorded transaction history can hardly be modified or all users agree on the same transaction history in a reasonable time.

Garay et al. (2015) are the first to analytically define system“reliability” using the concepts *common prefix property* and *chain quality property*. They show that Bitcoin possesses the two properties under the assumption that communication among participants is highly synchronized. In another study, Pass et al. (2017) allow for asynchronous communication with a bounded delay and find similar results. The subsequent discussion examines several streams of research related to our study of the interaction of participant decisions in a blockchain system.

2.1. Incentives and Participant Behavior

Miner Incentives and Decision Strategies: In the first study on blockchain miners' participation incentives, Kroll et al. (2013) show that the impact of transaction fees on miners' participation decisions is low when the block reward is high. They also find that transaction fees function as a reward substitute and impact miners' prioritization of transactions in the mempool.

Subsequent papers explore other determinants of miners' decisions. Prat and Walter (2018) conduct an empirical study on Bitcoin and establish a model to verify that miners' decisions are influenced by the exchange rate of the cryptocurrency to US dollars. In another study, Arnosti and Weinberg (2018) show that miners' participation decisions are affected by the required investment costs for mining machine and electricity. They further derive an equilibrium of miners' decisions under asymmetric investment costs and show how cost asymmetry leads to a market oligopoly. Finally, Cong et al. (2019) examine the impact of miner collaboration decisions, (i.e., miners pool their computing power together to form a so-called mining pool in order to reduce the risk of mining) on the extent of computing power decentralization.

User Behavior and Miner Participation Decisions: Another stream of research examines users' participation decision and bids on the transaction fees and how their decisions affect the miners' participation decisions. Huberman et al. (2021) and Easley et al. (2019) characterize the equilibrium of users' strategy under a priority queueing model. The difference between the two studies is that Huberman et al. (2021) assume that the block size can be any integer and optimize the block size to achieve the maximum total transaction fees. By contrast, Easley et al. (2019) only consider block size of one. Our study builds on the utility model from Huberman et al. (2021) while extends these models by modeling the interplay of user and miner decisions and the design of blockchain systems in greater detail, especially with miners' impacts on users through security concerns, and examining the reliability of decentralized payment systems under possible adversarial attacks.

Auction Mechanisms for Transaction Fees: Another stream of work related to our study focuses on the mechanism for determining transaction fees, comparing the performance of various auction mechanisms with the current "pay your bid" transaction fees mechanism. Within this area, Lavi et al. (2019), Yao (2018) and Basu et al. (2019) consider different auction mechanisms for determining transaction fees, while Lavi et al. (2019) show that their new mechanism can extract higher transaction fees from users.

Blockchain Related Research in Operations Management: Research on blockchain technology is still quite new in the field of operations management. One study in this area (Babich and Hilary (2019)) identifies five strengths and weaknesses in blockchain applications and points out several potential areas for future research. In another study, Cui et al. (2018) examine how improved traceability due to blockchain technology influences quality decisions and supply chain contracts in parallel and serial supply chains. Our study can lend potential insight into this emerging field within operations management research.

2.2. Priority Queues with Rational Behavior

In addition to the research on participant incentives, our study is related to the queueing literature, as we model the operations of Bitcoin as a priority queue and with rational participants. Within this area, Hassin (2016) provides a comprehensive review. Meanwhile, several studies on queues with priority and rational behavior are closely related. In an early study, Kleinrock (1967) investigates an unobservable $M/M/1$ queueing system in which a relative position in the queue is determined by a customer's bribe and establish the relationship between the bribe amount distribution and the average waiting time. When the cost is a heterogeneous linear combination of bribe amount and waiting time, they establish certain monotonicity in the optimal deterministic bribing under a constant average bribe constraint.

In two additional studies, Lui (1985) and Hassin (1995) analyze an $M/G/1$ queue in a similar setting while assuming a linear waiting cost and additive positive utility from receiving the service, each with a different linear coefficient distribution, to determine the impact of the process rate on revenue and social welfare. Since a low process rate creates less competition but a greater number of entrants, they aim for an optimal balance in their respective models. Our queueing model differs from theirs in that our transaction fee affects both the position of the customers and the equilibrium behavior of the miners (server), leading to a more involved influence on the waiting time of users.

3. Model Description

In this section, we outline a model that incorporates the operational features of blockchain systems as a payment service, the interplay between miners and users, and the security issue associated with the decentralized nature of the blockchain system.

In our model, transactions arrive to the system over time and are immediately placed in the mempool. Miners then select transactions from the mempool and process the transactions in blocks up to K transactions through a mining procedure, which is essentially a series of Bernoulli trials until one success. Thus, the number of trials needed to mine a block follows a geometric distribution and the service time can be described as an exponential random variable with rate μ. If we assume that transactions submitted by users arrive to the system according to a Poisson process with rate λ, then a blockchain system essentially operates as an $M/M/1$ queue with arrival rate λ, service rate μ, and batch size K. The service discipline is prioritized by the fee b that a user is willing to pay for his transaction to be processed, such that the higher the fee, the more quickly the transaction will be selected and processed.

We adopt the same utility function as used by Huberman et al. (2021) to model users' decision process, except that we assume a convex waiting cost and incorporate confirmation latency due to security requirement as part of the total waiting time. For each transaction processed, a user will gain R, pay a transaction fee b, and incur a waiting cost that is an increasing convex function $c(\cdot)$ of the total waiting time, i.e., the queueing latency plus the confirmation latency. Thus, some potential users may not join the system and the fees users are willing to pay may be different, depending on the system status upon arrival. Hence, we model a user's behavior by (p, G), where p is the probability a potential user will join the system and G is the cumulative distribution function from which the fee b is sampled. Assuming that the total market size is Λ, the arrival rate to the service system $\lambda = p\Lambda$ if every user joins the system with the same probability p. For generality, we allow the system to specify a minimum entrance fee $\underline{b}$, so the support of G is $[\underline{b}, \infty)$. In Section 6, we will extend our basic model to accommodate users with heterogeneous linear waiting cost functions or security requirements.

In our basic model, we assume away the block reward due to its planned disappearance in the mainstream cryptocurrencies. We further ignore potential miner incentives based on the market value of cryptocurrencies given the difficulty in modeling the volatility of these currencies. Thus, we assume that miners' total computing power is proportional to the total fee paid by users, Φ. Without loss of generality, we simply use Φ to represent the total computing power provided by miners. Note that miners' total computing power Φ does not affect the block production rate μ in practice as mining difficulty is dynamically adjusted with Φ. Hence, Φ affects neither the system capacity μK nor users' waiting time in the mempool.

By contrast, Φ does affect the confirmation latency required to guarantee that there is an overwhelmingly small probability of the system being attacked by an adversary, e.g., 10^{-4}. Although adversary's computing costs, i.e., electricity and operating costs, may be compensated by the gain from a successful attack, such a success is only possible after a heavy investment in acquiring computing power as argued by Budish (2018). As a matter of fact, adversary needs to out power honest miners in order to catch up and overtake the longest chain with a reasonable chance. Thus, the entry barrier is quite high for adversary, especially when Φ is high, and adversary's computing power is relatively low in reality. To avoid the complications of adversary's entry decision, we assume that the total mining power from adversary is known and fixed at A in a given period of time. A similar assumption is made in Pagnotta (2018) for studying the interplay between the Bitcoin price and system security.

Thus, a higher computing power Φ makes it more difficult for an adversary to overtake the longest chain and hence a shorter confirmation latency is required. If we let z denote the number of blocks required to be extended on the same branch to ensure a sufficiently low probability δ that a newly-mined block on the longest chain is confirmed, then it takes $\frac{z}{\mu}$ amount of time to confirm a block of transactions in expectation. For convenience, we refer to z as the *confirmation latency*, which is decreasing in miners' computing power Φ for a given δ. While z is an integer in practice, we treat it as a real number in our basic model for ease of presentation, and treat z as an integer in our extensions and numerical studies.

Figure 1 summarizes our basic model of how user behavior (p, G) and miners' total computing power Φ influence each other through total transaction fees and confirmation latency z. Miners' computing power Φ affects the confirmation latency z, which impacts users' waiting costs and behavior (p, G). On the other hand, users' behavior (p, G) determines the total transaction fee which in turn incentivizes miners' computing power Φ.

$$\begin{tikzcd}
\text{Users' behavior } (p, G) \arrow[r] & \text{Total fee } \Phi \arrow[d] \\
\text{Confirmation latency } z \arrow[u] & \text{Miners' computing power } \Phi \arrow[l]
\end{tikzcd}$$

Figure 1 Interplay between users and miners through total transaction fees and confirmation latency

Given the complexity of a blockchain system, we focus on the equilibrium behavior as in most existing studies of complex systems including blockchains and use superscript "$*$" to represent equilibrium values and functions. Note that we may add different arguments to the notation as needed when deriving equilibrium behavior to make the dependence of outcomes and parameters explicit.

4. Interplay between Users and Miners

In Section 4.1, we first investigate users' equilibrium behavior (p^*, G^*) under any given confirmation latency z, which leads to an equilibrium miner computing power $\Phi^*(z)$. In Section 4.2, we examine the minimum required confirmation latency $z^*(\Phi)$ to achieve a certain security level for given total computing power Φ. System equilibria, defined as (z^*, Φ^*), are obtained and presented in Section 4.3.

4.1. Users' Equilibrium Behavior

Before analyzing users' behavior for a given confirmation latency z, we need to obtain their expected total waiting time and define their utility.

4.1.1. Users' Expected Total Waiting Time and Utility Function. Since it takes $\frac{z}{\mu}$ amount of time to confirm a block in expectation, we only need to derive the queueing latency. As described in Section 3, queueing latency is the expected waiting time in an $M/M/1$ queue with arrival rate λ assuming all users follow the same strategy, service rate μ, block size K transactions, and a fee-based priority. To derive the queueing latency, we begin by considering a user with a transaction fee b. Given a transaction fee distribution $G(\cdot)$ adopted by all users, only $1 - G(b)$ portion of all transactions will have fees above b and hence a higher priority. This means that, assuming that transactions with the same fee will be selected by miners on a first-come-first-serve basis (in fact, any tie-breaking rule yields an identical analysis as long as the distribution function G is continuous), the user will be bumped in the priority only by those who arrive at a rate of $\lambda[1-G(b)]$. Thus, if $G(\cdot)$ is continuous, his expected queueing latency is the expected time it takes for an $M/M/1$ batch service queue with arrival rate $\tilde{\lambda} = \lambda[1-G(b)]$ to become empty for the first time upon his arrival, which is

$$W_q(\tilde{\lambda}) = \begin{cases} \frac{1}{(1-\theta)[\tilde{\lambda}-\mu(K+1)\theta^K]}, & \text{if } \tilde{\lambda} < \mu K, \\ \infty, & \text{otherwise,} \end{cases} \tag{1}$$

where $\theta \in (0,1)$ is the unique solution to $(\tilde{\lambda} + \mu)\theta - \tilde{\lambda} - \mu\theta^{K+1} = 0$, as given in Lemma A2 of Huberman et al. (2021).

We later demonstrate that the users' equilibrium fee distribution $G^*(\cdot)$ is indeed continuous and thus Equation (1) applies to our equilibrium solutions. The next proposition states how the queueing latency changes in users' behavior (p, G) and establishes that the inverse function $W_q^{-1}(\cdot)$ is well-defined, which is critical for identifying users' equilibrium behavior in Theorem 1.

Proposition 1. *$W_q(\tilde{\lambda})$ is strictly increasing convex for $\tilde{\lambda} \in [0, \mu K)$.*

Based on Proposition 1, the total expected waiting time for a transaction with fee b given other users' behavior (p,G) and confirmation latency z is $W(b|(p\Lambda,G),z) = W_q\left(p\Lambda[1-G(b)]\right) + \frac{z}{\mu}$. For a given z, the expected utility of a user who adopts the strategy (p,G) given everyone else's strategy (p',G') is then $U((p,G)|(p',G'),z) = p\int_{\underline{b}}^{\infty}[R-b-c(W(b|(p'\Lambda,G'),z))]dG(b)$, assuming the utility of those users who balk is zero. For a given confirmation latency z, we define users' equilibrium strategy (p^*,G^*) as one that maximizes a user's expected utility given that all other users apply the same strategy, i.e., it is a solution to $U((p^*,G^*)|(p^*,G^*),z) = \sup\limits_{(p,G)}\left\{U((p,G)|(p^*,G^*),z)\right\}$.

4.1.2. Users' Equilibrium Behavior (p^*,G^*).

Before deriving users' equilibrium strategy in Theorem 1, we demonstrate in Proposition 2 that the equilibrium fee distribution $G^*(\cdot)$ is continuous and hence Equation (1) applies.

PROPOSITION 2. *The equilibrium fee distribution $G^*(\cdot)$ is continuous on $[\underline{b},\infty)$.*

Intuitively, if the equilibrium fee distribution $G^*(\cdot)$ were not continuous and instead exhibited a jump at b, then a positive proportion of the transactions would incur b as a fee. However, this is impossible as an infinitesimal increase at b would allow a transaction to jump ahead of a positive proportion of the transactions and reduce its queueing latency by a non-infinitesimal amount; hence, no user would bid at b. The continuity of $G^*(\cdot)$ and monotonicity of $W_q(\cdot)$ in Proposition 1 lead to a unique equilibrium user strategy $(p^*(z),G^*(\cdot|z))$ for a given z as stated in Theorem 1.

THEOREM 1. *For a given z, there exists a unique equilibrium user strategy $(p^*(z),G^*(\cdot|z))$,*

$$p^*(z) = \min\left\{\frac{1}{\Lambda}W_q^{-1}\left(c^{-1}(R-\underline{b}) - \frac{z}{\mu}\right), 1\right\}, \tag{2}$$

$$G^*(b|z) = 1 - \frac{1}{p^*(z)\Lambda}W_q^{-1}\left(c^{-1}\left(c\left(W_q(p^*(z)\Lambda) + \frac{z}{\mu}\right) - (b-\underline{b})\right) - \frac{z}{\mu}\right). \tag{3}$$

Users' equilibrium strategy as a function of the confirmation latency reveals some interesting properties presented in Proposition 3. For instance, a shorter confirmation latency z will attract more users to join the system, which intensifies user competition and increases queueing latency, resulting in higher transaction fees. As one will see later in our numerical study in Section 7, users' equilibrium strategy and its properties obtained from our simple utility function fits the Bitcoin data nicely.

PROPOSITION 3. *The equilibrium solution given in Theorem 1 has the following properties.*

1. *$p^*(z)$ decreases in z;*
2. *$G^*(\cdot|z)$ stochastically decreases in z;*
3. *For a given z, $G^*(b|z)$ is strictly increasing convex in b before it reaches 1.*

By Theorem 1, a user's expected equilibrium utility then becomes:

$$U((p^*,G^*)|(p^*,G^*),z) = \max\left\{0, R-\underline{b}-c\left(W_q(\Lambda)+\frac{z}{\mu}\right)\right\}. \tag{4}$$

If $R-\underline{b}-c\left(W_q(\Lambda)+\frac{z}{\mu}\right)\geq 0$, a user can achieve a positive utility by bidding the minimum entrance fee $\underline{b}$ even if all users choose to participate. In this case, all users will indeed participate, i.e., $p^*(z)=1$, and achieve a positive utility $R-\underline{b}-c\left(W_q(\Lambda)+\frac{z}{\mu}\right)$. Otherwise, $p^*(z)<1$ and all users will have a zero utility. Thus, users' total expected utility is also a function of z in equilibrium and can be expressed as:

$$U^*(z) = \Lambda\max\left\{0, R-\underline{b}-c\left(W_q(\Lambda)+\frac{z}{\mu}\right)\right\}. \tag{5}$$

4.1.3. Total Fee Φ^*. In equilibrium, transactions arrive to the system at the rate $p^*(z)\Lambda$ with homogeneous users. By Theorem 1, the expected total fee rate paid by users is given by:

$$\Phi^*(z) = p^*(z)\Lambda\int_{\underline{b}}^{\infty} b dG^*(b) = p^*(z)\Lambda\min\left\{R, \underline{b}+c\left(W_q(\Lambda)+\frac{z}{\mu}\right)\right\} - \int_0^{p^*(z)\Lambda} c\left(W_q(\tilde{\lambda})+\frac{z}{\mu}\right)d\tilde{\lambda}, \tag{6}$$

which leads to Proposition 4.

Proposition 4. *$\Phi^*(z)$ is decreasing and* $\ln[\Phi^*(z)]$ *is decreasing concave in z.*

The expected total fee exhibits monotonicity because the participation probability $p^*(z)$ decreases and the fee distribution $G^*(\cdot|z)$ decreases stochastically in the confirmation latency z by Proposition 3. While $\Phi^*(z)$ is not concave in general, it is log-concave, which helps in establishing the system equilibria in Section 4.3.

4.2. Confirmation Latency

To obtain the equilibrium confirmation latency z^* for a given total fee, or equivalently the total miner computing power Φ, we first derive the probability of a successful attack by modelling the attack process as a random walk following the blockchain literature in Section 4.2.1. Since the exact expression for the probability of a successful attack is quite complex and difficult to analyze, we introduce a simple yet accurate approximation in Section 4.2.2.

4.2.1. Probability of a Successful Attack. An attack is successful when an adversary is able to fork another chain from a confirmed block in the longest chain, referred to as double spending, and eventually overtake the longest chain following Nakamoto (2008). Since a confirmed block in the longest chain, by definition, has already been followed by at least z blocks, an adversary needs to catch up with the longest chain from at least z blocks behind. Hence, the number of blocks by which the adversary chain is behind the longest one is a random walk with a one-step transition

β	0.10	0.15	0.20	0.25	0.30	0.35	0.40	0.45	0.50	0.55	0.60	0.65	0.70	0.75	0.80
z	5	7	8	11	13	17	21	26	34	44	58	80	114	170	277
$\underline{z}$	5	6	8	10	13	16	20	26	33	43	57	77	110	165	269
$z-\underline{z}$	0	1	0	1	0	1	1	0	1	1	1	3	4	5	8
$\bar{z}$	5	7	9	11	14	17	21	27	34	45	59	81	115	172	279
$\bar{z}-z$	0	0	1	0	1	0	0	1	0	1	1	1	1	2	2

Table 1 Confirmation latency z and their approximations $\underline{z}$ and $\bar{z}$

probability $\frac{\Phi}{A+\Phi}$ if the next block is added to the longest chain and $\frac{A}{A+\Phi}$ otherwise. Thus, the probability the adversary will ever catch up with the longest chain from at least z blocks behind is

$$\gamma(\beta,z)=e^{-z\beta}\left[\beta^z\sum_{k=0}^{z}\frac{z^k}{k!}+\sum_{k=z+1}^{\infty}\frac{(z\beta)^k}{k!}\right], \tag{7}$$

where $\beta\triangleq\frac{A}{\Phi}$ is the adversary-to-miner computing power ratio. The higher the β and/or the smaller the z is, the higher the probability that an adversary will be able to launch a successful attack. Lemma 1 provides the lower and upper bounds for this probability.

Lemma 1. *For any given $0\le\beta<1$, $\underline{\gamma}(\beta,z)\le\gamma(\beta,z)\le\bar{\gamma}(\beta,z)$ where*

$$\underline{\gamma}(\beta,z)=\frac{1}{2}\beta^z e^{z(1-\beta)} \text{ and } \bar{\gamma}(\beta,z)=\left[\frac{1}{2}+\frac{1}{\sqrt{2\pi z}}\left(\frac{2}{3}+\frac{1}{1-\beta}\right)\right]\beta^z e^{z(1-\beta)}.$$

4.2.2. Confirmation Latency and Its Approximations. The confirmation latency for a given security level δ and ratio of computing power β is the smallest integer z that satisfies $\gamma(\beta,z)\le\delta$. Due to the complexity of $\gamma(\beta,z)$, we will look for approximations inspired by the bounds in Lemma 1.

Lemma 2. *Denote $\underline{z}$ and $\bar{z}$ as the smallest z such that $\underline{\gamma}(\beta,z)\le\delta$ and $\bar{\gamma}(\beta,z)\le\delta$, respectively. Then, the difference between $\bar{z}$ and $\underline{z}$ decreases as δ becomes smaller.*

Numerical experiments for various values of β when $\delta=0.001$ in Table 1 demonstrate the accuracy of $\bar{z}$ and $\underline{z}$ as approximations. From Table 1, we can see that $\bar{z}$, $\underline{z}$ and z are very close especially when the proportion of adversary computing power β is not too high, which is in general true in reality. Similar results are observed for various δ, but not presented here.

Since both the bounds work well, we will use the lower bound $\underline{\gamma}(\beta,z)$ as a proxy for $\gamma(\beta,z)$ for its simplicity. Furthermore, we will treat z as a continuous variable in our basic model for a cleaner presentation. We will present the analytical results when z is an integer in the extensions in Section 6 and numerical studies in Section 7. With z being a non-negative real number and using $\underline{\gamma}(\beta,z)$ as a proxy for $\gamma(\beta,z)$, the equilibrium confirmation latency $z^*(\Phi)$ satisfies $\underline{\gamma}\left(\frac{A}{\Phi},z^*(\Phi)\right)=\delta$ which results in the following:

$$z^*(\Phi)=\frac{\ln(2\delta)}{1-\frac{A}{\Phi}+\ln\left(\frac{A}{\Phi}\right)}. \tag{8}$$

4.3. System Equilibria

We define system equilibrium as (z^*, Φ^*) that satisfies (6) and (8), which describe the dependency between the confirmation latency z and computing power Φ in equilibrium. We first present the following critical property.

PROPOSITION 5. *$\underline{\gamma}\left(\frac{A}{\Phi^*(z)}, z\right)$ is quasi-convex in z, where $\Phi^*(z)$ is given by* (6).

While it is harder for an adversary to attack a system successfully when the confirmation latency z is higher given a fixed level of computing power Φ by Proposition 4, the probability of a successful attack $\underline{\gamma}\left(\frac{A}{\Phi^*(z)}, z\right)$ is not monotonic in equilibrium. This is because enhancing security with a higher confirmation latency z increases users' total waiting time, discouraging users from joining the system or paying higher fees by Proposition 3. This in turn will reduce the total fee and equivalently lower computing power Φ^*. Thus, $\underline{\gamma}(\beta, z)$ may increase or decrease in z, depending on whether the loss of computing power dominates the enhancement of security via an increase in the confirmation latency z. As $\underline{\gamma}(\beta, z)$ is an exponential function in z for a fixed β, the former (latter) dominates and $\underline{\gamma}\left(\frac{A}{\Phi^*(z)}, z\right)$ increases (decreases) in z when z is large (small). Furthermore, the quasi-convexity of $\underline{\gamma}\left(\frac{A}{\Phi^*(z)}, z\right)$ leads directly to the possibility of the existence of up to two system equilibria. Thus a unique equilibrium occurs if and only if $\min_z \left\{\underline{\gamma}\left(\frac{A}{\Phi^*(z)}, z\right)\right\} = \delta$. Proposition 5 leads directly to Theorem 2.

THEOREM 2. *A system equilibrium (z^*, Φ^*) exists if and only if $\min_z \left\{\underline{\gamma}\left(\frac{A}{\Phi^*(z)}, z\right)\right\} \leq \delta$, in which case there can exist up to two equilibria.*

We next examine how the system evolves. Suppose that an equilibrium exists and the system starts with Φ^0 amount of computing power from miners. Then, users will respond with a strategy which results in a required confirmation latency $z^1 = z^*(\Phi^0)$, according to (6). Miners will then adjust their collective computing power to $\Phi^1 = \Phi^*(z^1)$, following (8), and the process continues as $z^{n+1} = z^*(\Phi^n)$ and $\Phi^{n+1} = \Phi^*(z^{n+1})$, $n = 0, 1, \cdots$. It is obvious that a system that begins in equilibrium remains so. Otherwise, the following proposition reveals the evolution of the blockchain system before it reaches an equilibrium.

PROPOSITION 6. *Suppose that there exist at most two equilibria (z_1^*, Φ_1^*) and (z_2^*, Φ_2^*) with $z_1^* \leq z_2^*$ and $\Phi_1^* \geq \Phi_2^*$. Then, the series (z^n, Φ^n) converges to (z_1^*, Φ_1^*) if $\Phi^0 > \Phi_2^*$ and to $(\infty, 0)$ if $\Phi^0 < \Phi_2^*$.*

Here, z_1^* and z_2^* are the solutions to $\underline{\gamma}\left(\frac{A}{\Phi^*(z)}, z\right) = \delta$. That is, a system will converge to (z_2^*, Φ_2^*) only if the system starts with it, making (z_2^*, Φ_2^*) an unstable equilibrium. Figure 2 plots the evolution of series (z^n, Φ^n) when there are two equilibria: z^n as a function of $\frac{A}{\Phi^{n-1}}$ (from (8)) and Φ^n as a function of z^n (from (6)). As defined earlier, the equilibria are the solutions to (6) and (8), represented by the intersecting lines in Figure 2. If $\Phi^0 > \Phi_2^*$, i.e., the system begins with sufficient computing power, it will converge to a stable equilibrium (z_1^*, Φ_1^*) through a virtuous cycle, as seen in Figure 2(a). Otherwise, the system will be locked in a vicious cycle and eventually dissolve, as seen in Figure 2(b). A system that begins with insufficient computing power requires a long confirmation latency, which in turn discourages users from participating or being willing to pay high fees, in turn discouraging miners participation. Thus, key to a successful launch of a new blockchain system is the ability to secure a sufficient amount of initial mining power.

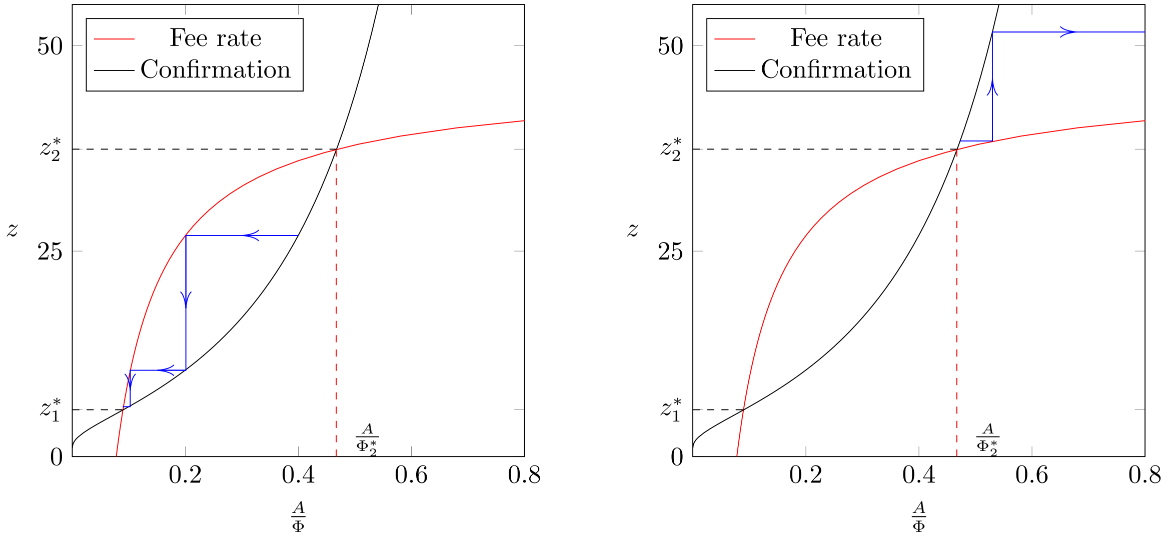

(a) Virtuous cycle ($\Phi^0 > \Phi_2^*$)

(b) Vicious cycle ($\Phi^0 < \Phi_2^*$)

Figure 2 **The evolution of a blockchain system for different levels of initial computing power** Φ^0

5. System Designs

While the potential market Λ, security level requirement δ, and amount of adversary computing power A are all exogenous, system designers are able to decide the rate μ at which blocks are created, the number of transactions K in a block, and the entrance fee $\underline{b}$. We refer to $(\mu, K, \underline{b})$ as a system design. Since each block must contain both transaction data and headers that identify the block in the entire blockchain, a small block size requires more headers and greater data storage. Coupled with other engineering concerns, we impose a lower bound K_m on the block size K and require that

$$K \geq K_m. \tag{9}$$

Furthermore, whenever a new block is mined, it is required to be broadcasted in the system, and the system capacity η, defined as the maximum number of transactions that can be broadcasted by the system per unit time, is fixed. Thus, given the rate at which blocks are created μ, the rate at which transactions can be processed is μK and we specify that

$$\mu K \leq \eta. \tag{10}$$

By Proposition 6, for any system design $(\mu, K, \underline{b})$, there may be two equilibria $(z_1^*, \Phi^*(z_1^*))$ and $(z_2^*, \Phi^*(z_2^*))$, and the latter can be reached only if the system beings with it and is unstable. Thus, we focus on the equilibrium $(z_1^*, \Phi^*(z_1^*))$ for any given system design. To indicate the dependence of performance on the design, we replace $p^*(z)$ in (2) with $p^*(z|\mu, K, \underline{b})$ and replace $\Phi^*(z)$ in (6) with $\Phi^*(z|\mu, K, \underline{b})$. Since an explicit expression for z_1^* as a function of $(\mu, K, \underline{b})$ is not available, we include z as a decision along with the design parameters $(\mu, K, \underline{b})$ where z satisfies the following security constraint

$$\underline{\gamma}\left(\frac{A}{\Phi^*(z|\mu, K, \underline{b})}, z\right) = \delta. \tag{11}$$

Thus, a feasible design $(\mu, K, \underline{b})$ and the corresponding confirmation latency z in equilibrium must satisfy (9), (10), and (11). We investigate optimal designs with the goals of maximizing the system equilibrium throughput in Section 5.1 and users' total utility in Section 5.2.

5.1. Maximizing the Throughput

Denoting the throughput rate as $\lambda^*(z|\mu, K, \underline{b}) = p^*(z|\mu, K, \underline{b})\Lambda$, we can express the optimization problem as follows:

$$\begin{aligned} \max_{(z,\mu,K,\underline{b})\geq 0} \quad & \lambda^*(z|\mu, K, \underline{b}) \\ \text{s.t.} \quad & (9), (10), (11). \end{aligned}$$

We first partially characterize an optimal solution in Lemma 3

Lemma 3. *For any feasible z, there exits $\underline{b}(z) \in \left[0, \left[R - c\left(W_q(\Lambda|\frac{\eta}{K_m}, K_m) + \frac{zK_m}{\eta}\right)\right]^+\right]$ such that $(\mu, K, \underline{b}) = \left(\frac{\eta}{K_m}, K_m, \underline{b}(z)\right)$ maximizes the throughput, if the feasible region is not empty.*

While Lemma 3 does not rule out other optimal designs, it establishes that there exists at least one optimal solution such that constraints (9) and (10) are binding, if the feasible set is not empty. Essentially, the solution entails setting a block size as small as possible and running the system at full capacity. Indeed, we observe smaller block sizes in practice, e.g., IOTA even sets $K = 1$ (Popov (2016)). Note that our finding that an optimal system should run at full capacity $\mu K = \eta$ differs from the conclusion in Huberman et al. (2021) that a blockchain system should withhold some capacity to create longer queues. This difference in conclusions reflects differences in the goals and decisions. First, while we maximize the throughput rate and specify that congestion discourages user participation, they maximize the transaction fees given a fixed arrival rate and specify that congestion motivates users to bid high fees. Second, they implicitly set $\underline{b}=0$ and ignore the security issue, while we treat $\underline{b}$ as a decision and require a confirmation latency z to address the security requirement, both of which can influence the fees. Their model can thus be viewed as a limiting case of ours when $R=\infty$ and $z=0$, under which maximizing the throughput is equivalent to maximizing the total fees and their solution is also feasible to our problem. We further note that while they maximize the total fees by congesting the system, we do so by setting a positive $\underline{b}$ to extract users' utility such that it motivates sufficient miner participation to ensure a secure system without diminishing the throughput rate.

By Lemma 3, we can now reduce the above optimization problem to the one that determines the confirmation latency z and an implicit function $\underline{b}(z)$ as

$$\max_{\underline{b}(z),z\geq 0} \quad \lambda^*\left(z\,\middle|\,\frac{\eta}{K_m},K_m,\underline{b}(z)\right) \tag{12}$$

$$\text{s.t.} \quad \underline{\gamma}\left(\frac{A}{\Phi^*\left(z|\frac{\eta}{K_m},K_m,\underline{b}(z)\right)},z\right)=\delta, \tag{13}$$

$$\underline{b}(z)\in\left[0,\left[R-c\left(W_q\left(\Lambda|\frac{\eta}{K_m},K_m\right)+\frac{zK_m}{\eta}\right)\right]^+\right]. \tag{14}$$

If $z\geq z_0$ where $R=c\left(W_q\left(\Lambda\middle|\frac{\eta}{K_m},K_m\right)+\frac{z_0K_m}{\eta}\right)$, then $R\leq c\left(W_q\left(\Lambda\middle|\frac{\eta}{K_m},K_m\right)+\frac{zK_m}{\eta}\right)$ and $\underline{b}(z)=0$ at which the objective function $\lambda^*\left(z\middle|\frac{\eta}{K_m},K_m,0\right)$ decreases in z from Λ. Otherwise, all users will participate and $\lambda^*\left(z\middle|\frac{\eta}{K_m},K_m,\underline{b}(z)\right)=\Lambda$, as discussed in Section 4.1.2. Thus, the optimal objective value (12) is exactly $\lambda^*\left(z\middle|\frac{\eta}{K_m},K_m,0\right)$. Since $\underline{\gamma}\left(\frac{A}{\Phi^*\left(z|\frac{\eta}{K_m},K_m,\underline{b}\right)},z\right)$ decreases in $\underline{b}$, feasibility of z in Problem (12)-(14) can be expressed by constraints (16) and (17) below, and Problem (12)-(14) is equivalent to the following problem with a single decision variable z as

$$\max_{z} \quad \lambda^*\left(z\,\middle|\,\frac{\eta}{K_m},K_m,0\right) \tag{15}$$

$$\text{s.t.} \quad \underline{\gamma}\left(\frac{A}{\Phi^*\left(z\middle|\frac{\eta}{K_m},K_m,\left[R-c\left(W_q(\Lambda|\frac{\eta}{K_m},K_m)+\frac{zK_m}{\eta}\right)\right]^+\right)},z\right)\leq\delta, \tag{16}$$

$$\underline{\gamma}\left(\frac{A}{\Phi^*\left(z|\frac{\eta}{K_m},K_m,0\right)},z\right)\geq\delta. \tag{17}$$

We first establish that the left-hand sides of (16) and (17) are quasi-convex in Lemma 4.

Lemma 4. *Both* $\underline{\gamma}\left(\frac{A}{\Phi^*\left(z\middle|\frac{\eta}{K_m},K_m,\left[R-c\left(W_q\left(\Lambda\middle|\frac{\eta}{K_m},K_m\right)+\frac{zK_m}{\eta}\right)\right]^+\right)},z\right)$ *and* $\underline{\gamma}\left(\frac{A}{\Phi^*\left(z\middle|\frac{\eta}{K_m},K_m,0\right)},z\right)$ *are quasi-convex in* z.

If the feasible region defined by (16) and (17) is non-empty, there exist z_3 and z_4, $z_3 \le z_4$, such that (16) is binding. Furthermore, if there exist z_3' and z_4', $z_3' \le z_4'$, such that equality holds in (17), then it is easy to verify that $z_3 \le z_3' \le z_4' \le z_4$. Thus, the feasible region is either $[z_3, z_3'] \cup [z_4', z_4]$ or $[z_3, z_4]$ and any feasible z, $z \le z_0$, is optimal. We summarize the structure of the optimal solutions in the next proposition.

Proposition 7. *If the feasible region of* (15)–(17) *is not empty,* z_3 *is always optimal.*

1. *If* $z_0 < z_3$, $(z,\mu,K,\underline{b}) = (z_3, \frac{\eta}{K_m}, K_m, 0)$ *is the unique optimal solution and the optimal* $\lambda^*\left(z_3\middle|\frac{\eta}{K_m},K_m,0\right) < \Lambda$.
2. *Otherwise, the set of optimal solutions is* $[z_3, z_0 \wedge z_3']$ *or* $[z_3, z_0 \wedge z_4]$ *and* $\lambda^*\left(z\middle|\frac{\eta}{K_m},K_m,0\right) = \Lambda$.

Note that there may be multiple solutions that lead to the maximum throughput Λ. Indeed, with a sufficiently high utility gain R, $K > K_m$, $\mu = \frac{\eta}{K}$, and $\underline{b} = 0$ may also yield the maximum throughput Λ. However, when the objective is to maximize users' total utility, there exists a unique optimal solution, as we discuss next.

5.2. Maximizing Users' Total Utility

Since the miners achieve zero utility in a completely competitive environment, maximizing users' total utility (5) and maximizing the social welfare are equivalent in our setting. Furthermore, users' total utility is also zero when $\lambda^* < \Lambda$, say $p^* < 1$, as shown in Section 4.1. Thus, the designs that maximize users' utility must be among those that achieve the throughput Λ, i.e.,

$$p^*(z|\mu, K, \underline{b}) = 1. \tag{18}$$

To indicate the dependence explicitly, we use $U^*(z|\mu,K,\underline{b})$ and $W_q(\Lambda|\mu,K)$ to represent users' total utility and waiting time, respectively. At $p^* = 1$, the objective function reduces to:

$$U^*(z|\mu,K,\underline{b}) = \Lambda\left[R - \underline{b} - c\left(W_q(\Lambda|\mu,K) + \frac{z}{\mu}\right)\right]. \tag{19}$$

We can now describe the problem as follows:

$$\begin{aligned} \max_{(z,\mu,K,\underline{b})\ge\mathbf{0}} \quad & U^*(z|\mu,K,\underline{b}) \\ \text{s.t.} \quad & (9), (10), (11), (18). \end{aligned}$$

The feasible region of the above problem is a subset of the feasible region when maximizing throughput. While a solution where constraints (9) and(10) are not binding may also be optimal when the goal is to maximize throughput, when the goal is to optimize user utility, a system designer must use up all system capacity and set the block size as small as possible, as indicated in Lemma 5.

LEMMA 5. *Suppose that the feasible region is not empty. Then, an optimal solution must exist and be of the form* $(z^*, \mu^*, K^*, \underline{b}^*) = \left(z^*, \frac{\eta}{K_m}, K_m, \underline{b}(z^*)\right)$.

This is because, for any feasible solution $(z, \mu, K, \underline{b})$, a feasible solution $\left(z, \frac{\eta}{K_m}, K_m, \underline{b}(z)\right)$ will increase user utility by reducing the waiting cost while maintaining the total transaction fee. Thus, there exists a unique optimal design for a given z. By Proposition 7, the problem to maximize users' utility can be reduced to the following unconstrained form:

$$\max_{z\geq 0} \; U^*\left(z \middle| \frac{\eta}{K_m}, K_m, \underline{b}(z)\right) \tag{20}$$

$$\text{s.t.} \quad z \in [z_3, z_0 \wedge z_3']. \tag{21}$$

By equations (6) at $p^*(z) = 1$ and (8), $U^*\left(z \middle| \frac{\eta}{K_m}, K_m, \underline{b}(z)\right)$ can be written as a function of Φ^* as

$$U^*(\Phi^*) = \Lambda R - \Phi^* - \int_0^\Lambda c\left(W_q\left(\tilde{\lambda} \middle| \frac{\eta}{K_m}, K_m\right) + \frac{\ln(2\delta)}{\frac{\eta}{K_m}\left[1 - \frac{A}{\Phi^*} + \ln(\frac{A}{\Phi^*})\right]}\right) d\tilde{\lambda}. \tag{22}$$

This leads to Lemma 6.

LEMMA 6. *$U^*(\Phi^*)$ is quasi-concave with a unique maximizer $\hat{\Phi}^*$ and $z^*(\hat{\Phi}^*) \geq z_3$.*

When the computing power Φ^* is low, the required confirmation latency is long and the waiting cost in (22) is high, resulting in lower user utility. However, when Φ^* is high, users pay high fees, which also yields lower utility. The quasi-concavity of $U^*(\Phi^*)$ leads to a unique optimal confirmation latency for Problem (20)-(21).

PROPOSITION 8. *The unique optimal $z^* = z_0 \wedge z_3' \wedge z^*(\hat{\Phi}^*)$.*

Here, z_0 enforces a throughput rate of Λ, z_3' fulfils the security requirement, and $z^*(\hat{\Phi}^*)$ is the unique maximizer of the utility function.

6. Extensions

We present the results when the confirmation latency z is an integer in Section 6.1, extend our basic model to allow a block reward to each winning miner for creating a block besides the transaction fees in Section 6.2, and derive users' equilibrium strategy under heterogeneous user waiting costs and security requirements in Section 6.3.

6.1. Confirmation Latency z as an Integer

We first consider the implications for our model when we treat the confirmation latency z as an integer rather than a real number. Theorem 3 presents the set of equilibria confirmation latencies obtained through establishing the quasi-convexity of $\underline{\gamma}\left(\frac{A}{\Phi^*(z)}, z\right)$ and $\underline{\gamma}\left(\frac{A}{\Phi^*(z)}, z-1\right)$. Here, the equilibrium behaviors identified in Theorem 2 and Proposition 6, are replaced by Theorem 3 and Proposition 9, respectively. Recall that z_1^* and z_2^* are defined in Proposition 6 and the solutions to $\underline{\gamma}\left(\frac{A}{\Phi^*(z)}, z\right) = \delta$, given that these solutions exist. Let z_1' and z_2' be the solutions to $\underline{\gamma}\left(\frac{A}{\Phi^*(z)}, z-1\right) = \delta$ if they exist. Then, $\lceil z_1^* \rceil < z_1' \leq z_2' \leq z_2^*$.

Theorem 3. *An equilibrium z^* exists if and only if $\min_{z \in \mathcal{N}^+} \underline{\gamma}\left(\frac{A}{\Phi^*(z)}, z\right) \leq \delta$, in which case the system equilibria are all the integers in $[z_1^*, z_2^*]$ if $\min_{z \in \mathcal{N}^+} \underline{\gamma}\left(\frac{A}{\Phi^*(z)}, z-1\right) > \delta$ or $[z_1^*, z_2^*]/[z_1', z_2']$ otherwise.*

Recall that, when z is treated as a real number, the set of equilibria, if exists, is reduced by up to two points z_1^* and z_2^* as stated in Theorem 2. As long as an equilibrium exists when z is treated as a real number, $\lceil z_1^* \rceil < z_1'$ guarantees the existence of an integer equilibrium. Analogous to Proposition 6, we now consider the series defined by $z^{n+1} = \lceil z^*(\Phi^{n+1}) \rceil = \left\lceil \frac{\ln 2\delta}{1 - \frac{A}{\Phi^n} + \ln \frac{A}{\Phi^n}} \right\rceil$ and $\Phi^{n+1} = \Phi^*(z^{n+1})$ with initial computing power Φ^0. When the set of equilibria is comprised of all the integers in $[z_1^*, z_2^*]/[z_1', z_2']$, the system will evolve through either a vicious or virtuous cycle, as stated in Proposition 9.

Proposition 9. *Suppose the set of equilibria z is all the integers in $[z_1^*, z_2^*]/[z_1', z_2']$.*

1. *If $z_1^* \leq \lceil z^*(\Phi^0) \rceil < z_1'$ or $z_2' < \lceil z^*(\Phi^0) \rceil \leq z_2^*$, the system begins and remains at an equilibrium.*
2. *Otherwise, the series z^n converges to $\lceil z_1^* \rceil$ if $\lceil z^*(\Phi^0) \rceil < z_1^*$, to $\lceil z_1' - 1 \rceil$ if $z_1' \leq \lceil z^*(\Phi^0) \rceil \leq z_2'$ and to ∞ in which case $\Phi^* = 0$ if $\lceil z^*(\Phi^0) \rceil > z_2^*$.*

6.2. Existence of Block Rewards and Confirmation Latency as an Integer

Suppose that miners also receive a reward B for each block mined or $B_0 = \mu B$ per unit time. Then, the miners' total fee, or equivalently their total computing power, in equilibrium becomes $B_0 + \Phi^*$ per unit time. Furthermore, the probability of a successful attack $\underline{\gamma}\left(\frac{A}{\Phi^*(z)+B_0}, z\right)$ is no longer quasi-convex in z in general, as shown numerically in Section 7.3. While a structural analysis of the equilibrium behavior becomes very difficult, we are able to derive the structure of the optimal design in Propositions 10 and 11 as counterparts of the design outlined in Propositions 7 and 8.

Here, it is easy to verify that Lemma 3 still holds, with the exception that $\underline{b}(z)$ may not be unique, so the problem with the goal of maximizing throughput rate can still be reduced to a problem with a single decision variable z.

Proposition 10. *When the feasible region of the problem with the goal of maximizing the throughput rate in the presence of a block reward is non-empty and $\tilde{z}_3$ is the smallest feasible integer, the following will hold.*

1. *If $\lambda^*\left(\tilde{z}_3|\frac{\eta}{K_m},K_m,0\right)<\Lambda$, then $(z,\mu,K,\underline{b})=\left(\tilde{z}_3,\frac{\eta}{K_m},K_m,0\right)$ is the unique optimal solution.*
2. *Otherwise, there exists $\tilde{z}_4$, $\tilde{z}_4\geq\tilde{z}_3$, such that $\left(z,\frac{\eta}{K_m},K_m,\underline{b}(z)\right)$ is optimal for all $z\in[\tilde{z}_3,\tilde{z}_4]$ and $\lambda^*\left(z,\frac{\eta}{K_m},K_m,\underline{b}(z)\right)=\Lambda$.*

In the absence of a block reward, $\tilde{z}_3=\lceil z_3\rceil$ where z_3 is defined as in Proposition 7. Recall that $z^*(\hat{\Phi}^*)$ is defined in Lemma 6.

Proposition 11. *In the presence of a block reward, a design that maximizes users' utility must be in the form $(z,\mu,K,\underline{b})=\left(z,\frac{\eta}{K_m},K_m,\underline{b}(z)\right)$ where the optimal z is $\tilde{z}_4\wedge\lceil z^*(\hat{\Phi}^*)\rceil$ and/or $\tilde{z}_4\wedge\lfloor z^*(\hat{\Phi}^*)\rfloor$.*

6.3. Users Heterogeneity

In our final extension of our model, we consider the impact of heterogeneity in users' waiting costs and security requirements on the equilibrium behavior.

6.3.1. Heterogeneous Waiting Costs. We follow Huberman et al. (2021) and allow users to have different waiting costs, i.e., a user's waiting cost is a linear function $c(w)=Cw$ where C follows a general distribution and is not required to be continuous. Since there may be infinite types of users, it is difficult to derive an equilibrium behavior for each type of user. Thus, we derive an aggregated participation probability p^* and fee distribution $G^*(\cdot)$ in equilibrium for a given z, and the resulting computing power Φ^*.

We outline the aggregated equilibrium user strategy in Proposition 12. The key insight is that the q% of users who are most patient will pay the q% lowest fees.

Proposition 12. *Let $C(q)$ and $b(q)$ be the q-quantile of the their respective distributions, respectively. Then,*

$$
\begin{aligned}
p^* &= \max_{p'\leq 1}\left\{p':R-\underline{b}-\int_{p=0}^{p'}C(p'-p)dW_q(p\Lambda)-C(p')\left(\frac{1+z}{\mu}\right)\geq 0\right\},\\
b(q) &= \underline{b}+\int_{p=(1-q)p^*}^{p^*}C(p^*-p)dW_q(p\Lambda),\\
\Phi^* &= \underline{b}p^*\Lambda+\int_{p=0}^{p^*}p\Lambda C(p^*-p)dW_q(p\Lambda).
\end{aligned}
$$

6.3.2. Heterogeneous Security Requirements. In practice, confirmation latency of a transaction is an agreement between the seller and buyer involved in that particular transaction, reflecting heterogeneous user risk attitude. For instance, an optimistic seller may deliver the goods once the payment transaction is added to a block on the longest chain, while a conservative seller prefers to wait until a large number of blocks are subsequently added to guarantee a small chance of adversary attack. Thus, instead of assuming a deterministic δ across all users, we allow users' required security level Δ to be i.i.d. random variables drawn from a continuous cdf with support $[0, \bar{\delta}]$, where $0 < \bar{\delta} \ll 1$. Then, for a given level of miners' computing power Φ, confirmation latency is a random variable $Z^* = \frac{\ln(2\Delta)}{1 - \frac{A}{\Phi} + \ln\left(\frac{A}{\Phi}\right)}$. Proposition 13 presents the aggregated equilibrium strategy for users who decide to join the system. Similar to Proposition 12, the key insight here is that a high user security requirement is associated with a high fee due to the convexity of the waiting cost function $c(\cdot)$.

Proposition 13. *Let $\Delta(q)$ and $b(q)$ be the q-quantile of their respective distributions. Then,*

$$p^* = \max_{p' \leq 1} \left\{ p' : R - \underline{b} - \int_{p=0}^{p'} c'\left(W_q(p\Lambda) + \frac{\ln\left[2\Delta(1-p^*+p)\right]}{\mu\left[1 - \frac{A}{\Phi} + \ln\left(\frac{A}{\Phi}\right)\right]} \right) dW_q(p\Lambda) - c\left(\frac{1}{\mu} + \frac{\ln\left[2\Delta(1-p')\right]}{\mu\left[1 - \frac{A}{\Phi} + \ln\left(\frac{A}{\Phi}\right)\right]} \right) \geq 0 \right\},$$

$$b(q) = \underline{b} + \int_{p=(1-q)p^*}^{p^*} c'\left(W_q(p\Lambda) + \frac{\ln\left[2\Delta(1-p^*+p)\right]}{\mu\left[1 - \frac{A}{\Phi} + \ln\left(\frac{A}{\Phi}\right)\right]} \right) dW_q(p\Lambda),$$

and the resulting total transaction fee is

$$\Phi^* = \underline{b}p^*\Lambda + \int_0^{p^*\Lambda} p\Lambda c'\left(W_q(p\Lambda) + \frac{\ln\left[2\Delta(1-p^*+p)\right]}{\mu\left[1 - \frac{A}{\Phi} + \ln\left(\frac{A}{\Phi}\right)\right]} \right) dW_q(p\Lambda).$$

7. Numerical Study

In this section, we first use data from Bitcoin to verify our users' utility function (4.1.1) in Section 7.1 and equilibrium behavior obtained in Section 4 in Section 7.2. We then continue with a comprehensive illustration of optimal system design predicted by our models when the confirmation latency is an integer and miners are able to receive a block reward in Section 7.3.

In a blockchain system, transaction records are kept by all the miners and can be obtained from any miner. We crawl from a miner's website (`https://www.blockchain.com`) all the transaction data from the period of 16:28:18 Jan 5 to 23:59:59 January 31, 2018, which represents Bitcoin's most congested transaction period to date and hence contains transactions with the most significant fees. For each transaction, we obtain its *arrival time*, *size* in bytes, and *fee* in Satoshis, the smallest unit of Bitcoin currency (1 Bitcoin $= 10^8$ Satoshis), as well as the time that the block containing it was created. We extract the following system parameters from the data.

1. Arrival rate: Our dataset is comprised of a total of $6,674,639$ transaction arrivals, of which $6,669,963$ were successfully packed into a block by the end of the considered period, yielding an effective arrival rate $\lambda^* \approx 3.0518$ per second.
2. Process rate: Within our dataset, there is a total of $4,073$ created blocks, reflecting an average mining rate $\mu \approx 0.0018754$ blocks per second, or one every 9 minutes on average.
3. From Figure 3, the sizes of most transactions are concentrated around the median value of 226 bytes. Since the size limit of a block is 10^6 bytes by design, the block size $K \approx 10^6/226 = 4,425$ transactions.
4. Between 2016 and 2020,the block reward is $B = 12.5$ newly-minted Bitcoin, or 12.5×10^8 Satoshi. Since the transaction fees are in Satoshis per byte, the block reward rate $B_0 = \mu B = 12.5 \times 10^8 \times 0.0018754/226 = 10,370.57522$ Satoshis per second per byte, where 226 is the median transaction size.

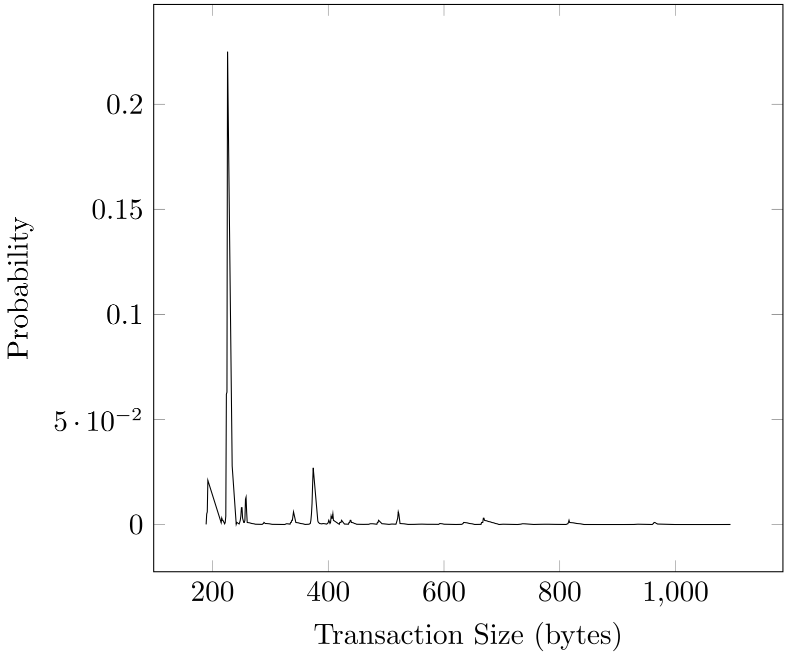

Figure 3 **Distribution of the transaction size**

With the above estimated parameters, we can estimate the parameters in the users' utility function in section 7.1. As we do not have access to more data needed to estimate other parameters, we will make the following assumptions for illustration purposes:

1. $z^* = 6$ as suggested in Nakamoto (2008);
2. The system runs at its capacity during our sample period, i.e., $\eta \approx \mu K = 8.24622$ transactions per second;

3. $\Lambda = 5.5$ per second so that $\lambda^* = 3.0518 < \Lambda < \eta = 8.24622$, the system capacity; and
4. $\delta = 10^{-4}$ and $10 \leq K_m \leq 4,000$.

7.1. Model Validation

Note that we describe users' utility with a very simple utility function:

$$U((p,G)|(p,G),z) = p\int_{\underline{b}}^{\infty}[R - b - c(W(b|(p\Lambda,G),z))]dG(b).$$

To verify whether this function captures users' behavior within the Bitcoin system, we further limit the waiting cost to be a linear function as $c(W) = CW$, i.e, our utility function has only two parameters (C,R). Using the data, we estimate $C = 2.079$ Satoshis per second per byte and $R = 8,270$ Satoshis per byte in the utility function by Theorem 1. Figure 4 plots the fee distribution $G^*(b)$ from the data marked as Empirical.

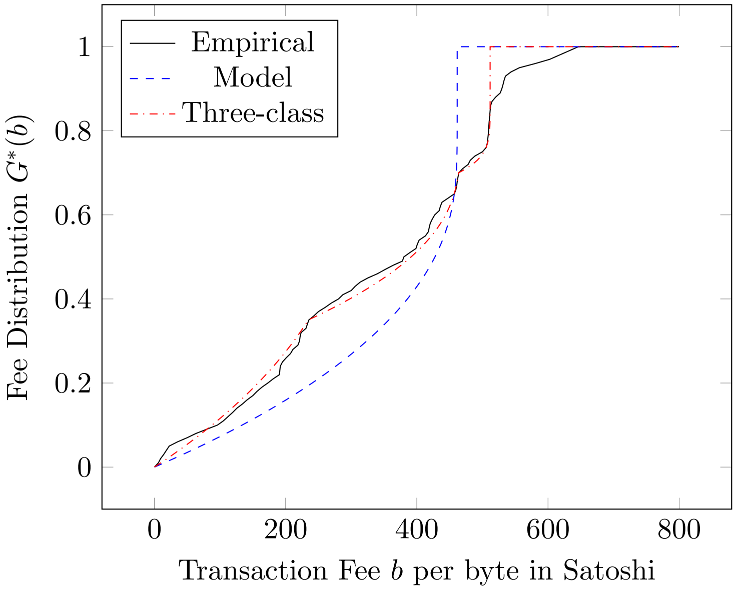

Figure 4 Distributions of fees

We then plot in Figure 4 the equilibrium fee distribution predicted by our model labeled as Model. As one can see, our simple model with only two degrees of freedom fits the data with only slight discrepancies which may be caused by user heterogeneity and behavior not captured by the model. Figure 4 further plots the fee distribution predicted by our model with three user classes (high with a waiting cost rate of 4.6281; medium, 2.424; and low, 1.3650), labeled as Three-class, and it clearly fits the data better. However, for simplicity, we will assume homogeneous users with $C = 2.079$ in our subsequent numerical study.

7.2. Equilibrium Behavior without Block Rewards

Given the utility function with $(C,R) = (2.079, 8, 270)$, $\mu = 0.0018754$, and $K = 4,425$, as estimated from the data, we can illustrate the extent to which users' equilibrium behavior $(p^*, G^*(b))$ and miners' computing power Φ^* change in z, predicated qualitatively in Proposition 3. From Figure 5(a), we can see that p^* hovers briefly at 1 before decreasing sharply to zero. Figure 5(b) illustrates how the increasing convex function $G^*(b)$ stochastically decreases in z and Figure 5(c) shows the log-concavity of Φ^*, while Figure 5(d) reveals that Φ^* at first exhibits a concave shape but becomes convex as z increases.

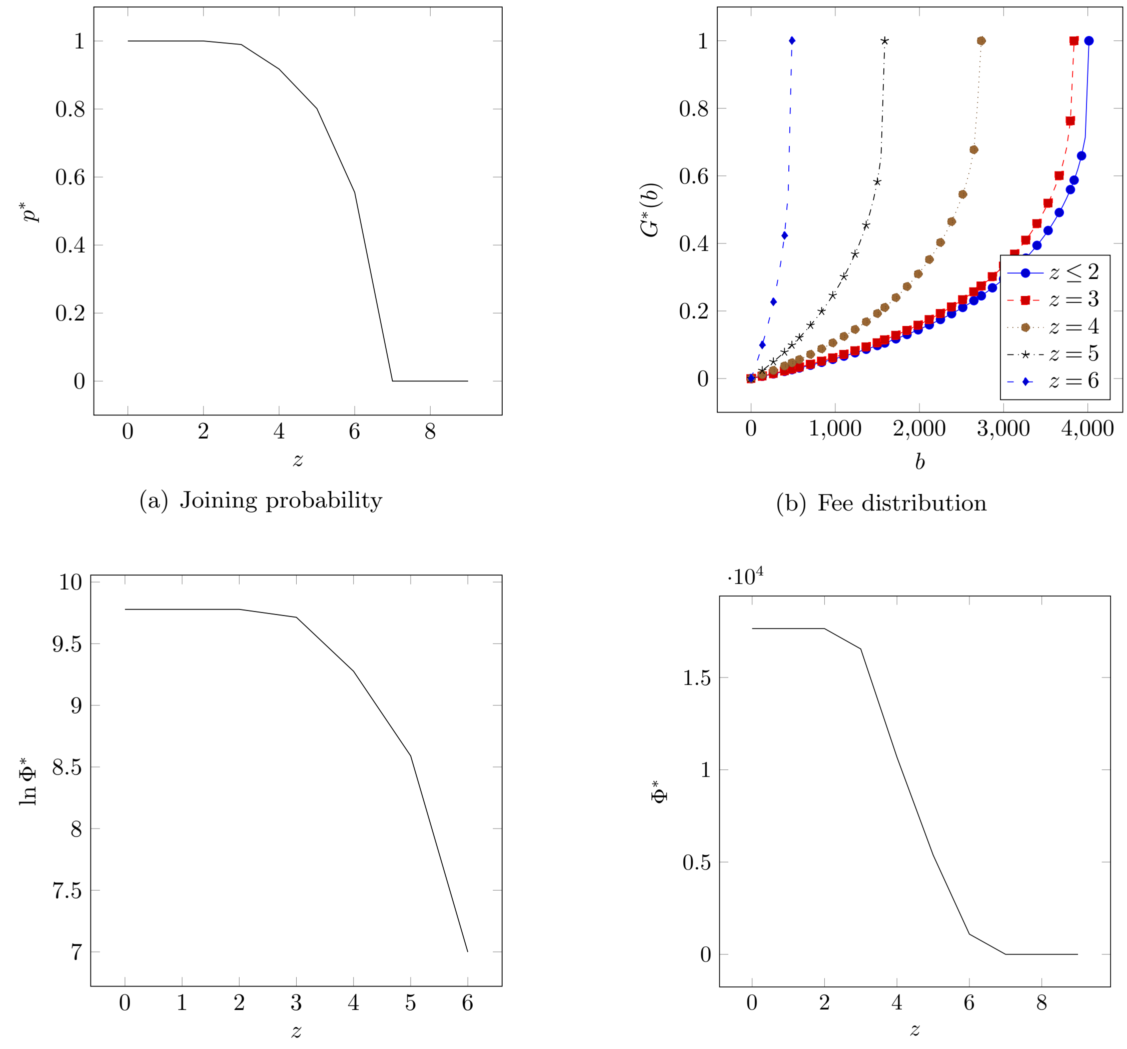

(a) Joining probability

(b) Fee distribution

(c) Log-concavity of the computing power

(d) Computing power

Figure 5 **Equilibrium user behavior for various z**

7.3. The Impact of a Block Reward to the Probability of a Successful Attack

We next use the Bitcoin data to examine the impact of a block reward on the probability that an adversary will launch a successful attack. At $B_0 = 10,370$ Satoshis per second per byte, the total computing power becomes $\Phi^* + B_0$. Here, we examine how the block reward affects the shape of the probability of a successful attack $\underline{\gamma}\left(\frac{A}{\Phi^*(z)+B_0}, z\right)$ as well as its sensitivity in A and z.

Although we cannot observe A, we can derive the upper bound allowed for any given δ. At $B_0 = 10,370$ and $z^* = 6$, the total fee $\Phi^*(6) = 1,095.3802$ Satoshis per second per byte and $\underline{\gamma}\left(\frac{A}{\Phi^*(z)+B_0}, z\right) \leq \delta = 10^{-4}$ implies $A \leq 9.81\%[\Phi^*(z) + B_0] = 1,124.8032$, indicating an extremely reliable system. By contrast, when there is no block reward, $A \leq 107.456798$, a much stronger requirement.

Figure 6 plots $\underline{\gamma}\left(\frac{A}{\Phi^*(z)+B_0}, z\right)$ as a function of z for various values of A. From Figure 6, we can see that the attack probability function is no longer convex. Figure 7 plots the equilibrium z^* in integers required as a function of δ for $A = 700$ and $1,000$. Here, the equilibrium z^* is always unique for $A = 700$; for $A = 1000$, it is unique except when $4.88 \times 10^{-5} \leq \delta \leq 4.96 \times 10^{-5}$ (between the dashed lines). As the figure shows, while z^* is quite sensitive to the hashing power of the adversary A for a given δ, it is not as sensitive to the security requirement δ for a given A. For instance, z^* changes from 8 to 5 as δ changes from 3×10^{-7} to 3×10^{-5} when $A = 700$ and from 6×10^{-6} to 10^{-4} when $A = 1,000$.

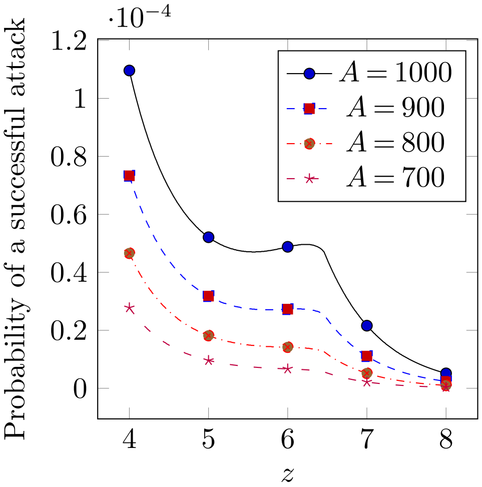

Figure 6 **Probability of a successful attack as a function of z for different A**

However, $\underline{\gamma}\left(\frac{A}{\Phi^*(z)+B_0}, z\right)$ is no longer quasi-convex in general in the presence of a block reward. Finally, we depict the probability of a successful attack since Bitcoin's inception in Figure 8 where $B_0 = 41,480$ (2008 - 2012, the initial reward), $10,370$ (2016 - 2020), $5,185$ (2020 - 2024), and 648

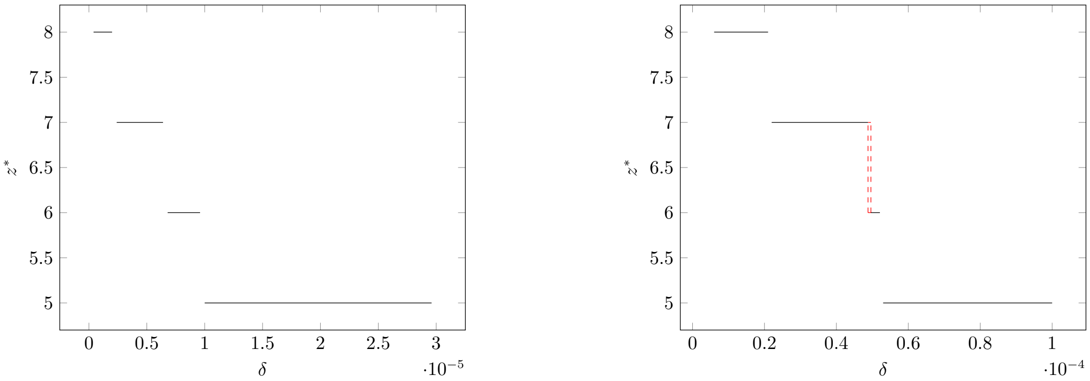

(a) $A = 700$

(b) $A = 1000$

Figure 7 **Integer equilibria z^* as δ varies**

(2032 - 2036) Satoshis per second per byte, assuming $A = 1,000$. As we can see, Proposition 5 and Theorem 2 no longer hold as the curves are not quasi-convex in general. From Figure 8, we identify the following properties of the probability function. (1) When the block reward is large enough, $\frac{A}{\Phi^*(z)+B_0}$ is dominated by $\frac{A}{B_0}$ and increasing z decreases $\underline{\gamma}\left(\frac{A}{\Phi^*(z)+B_0}, z\right)$. Thus, the probability of a successful attack is a decreasing function in z. (2) When the block reward is small enough, $\frac{A}{\Phi^*(z)+B_0}$ is dominated by $\frac{A}{\Phi^*(z)}$ and $\underline{\gamma}\left(\frac{A}{\Phi^*(z)+B_0}, z\right)$ is quasi-convex. (3) Otherwise, $\underline{\gamma}\left(\frac{A}{\Phi^*(z)+B_0}, z\right)$ may have several reflection points.

7.4. System Design

In our final numerical analysis, we illustrate our system design recommendations using Bitcoin Data. Assuming that Bitcoin runs at its capacity at $\eta = 8.24622$, we calculate the optimal equilibrium z^* as integers and the corresponding $\underline{b}(z^*)$ for K_m from 10 to $4,000$ at the block reward $B_0 = 10,370$ in Figure 9 and at $B_0 = 5,185$ (the current level) in Figure 10. Note that the shaded areas represent multiple equilibrium solutions that maximize the throughput while the solid lines represent the unique solutions that maximize the user utility. From Figures 9 and 10, we can see that as K_m increases and $\mu^* = \frac{\eta}{K_m}$ decreases, the shaded areas become narrower. As μ^* decreases, the time to process a block and the queueing latency both increase. This discourages miner participation and pushes down $\underline{b}(z^*)$, resulting in an increase in the lower bands of the areas and a decrease in the upper bands. Due to the high block reward and low $\underline{b}(z^*)$ (at zero most of the time), our z^* that maximizes the user utility occurs more often in the upper band.

8. Conclusions

In this paper, we develop a model to study the interplay between user participation and transaction fees, and miner participation in the presence of security concerns due to decentralisation. We

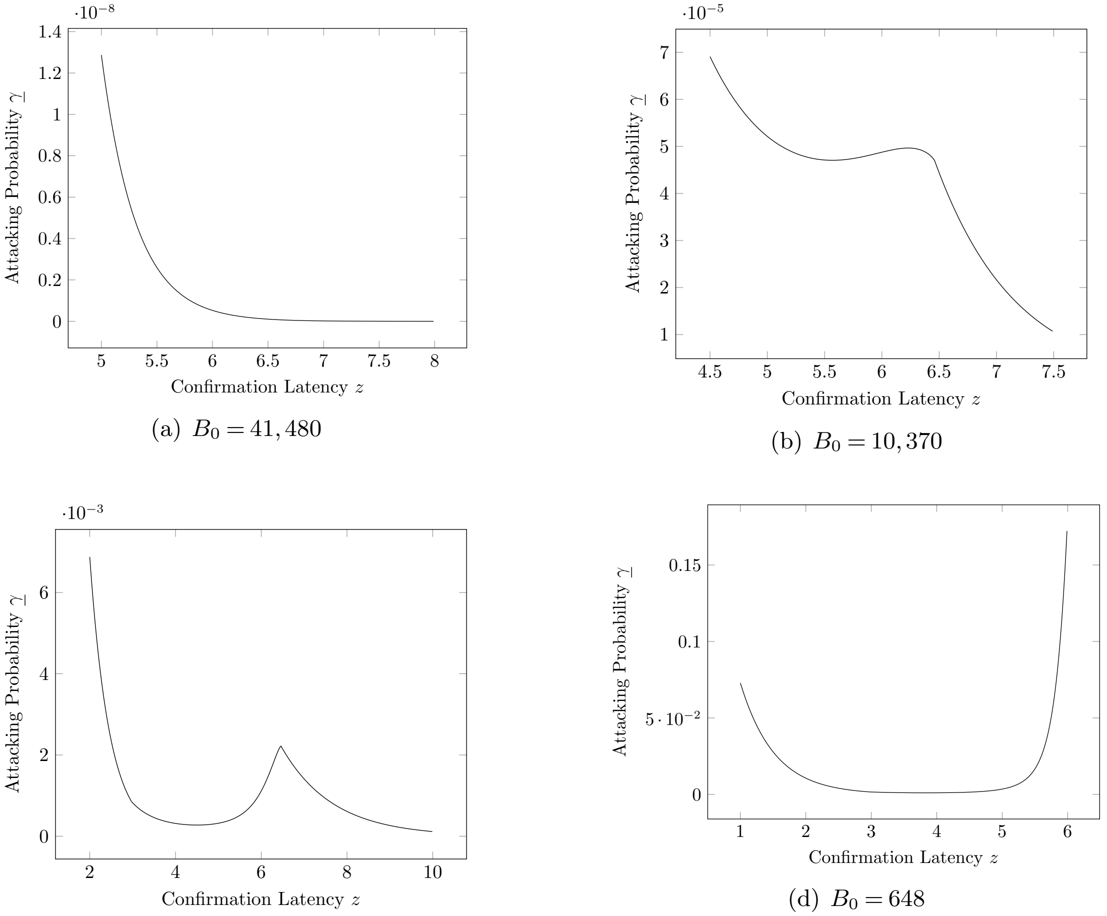

(a) $B_0 = 41,480$

(b) $B_0 = 10,370$

(c) $B_0 = 5,185$

(d) $B_0 = 648$

Figure 8 The probability of a successful attack for various block rewards B_0

analyze the equilibrium behavior of users and miners, and identify optimal designs in terms of the service rate, batch size, and entrance fee, that maximize system throughput and users' total utility. We validate our simple user utility function, a critical part of our model, using a sample data from Bitcoin.

Our equilibrium analyses reveal that the system must attract a sufficient level of initial computing power to encourage users to participate and pay high fees, which in turn motivates enough miners to participate, creating a virtuous cycle and a healthy system. Our analysis also provides insights into the optimal system design. In particular, there exists an optimal design that entails setting the block size as small as possible, consistent with practice trend, and running at full capacity, which contradicts previous research aiming at maximizing miners' revenue.

Future research may allow miners to have heterogeneous mining equipment setup and/or electricity costs. It is also interesting to study blockchain systems with functions beyond cryptocurrencies

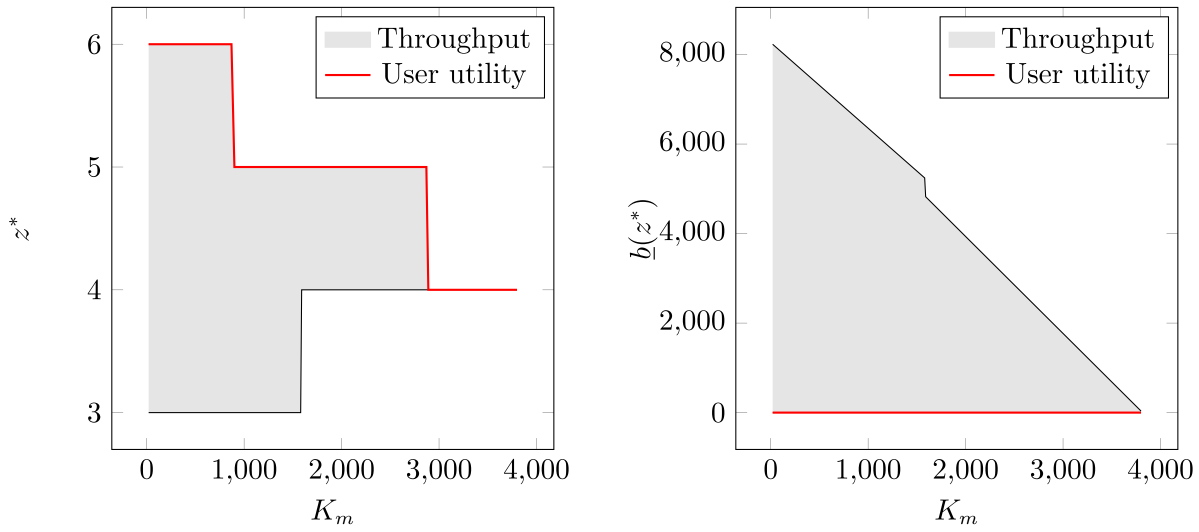

Figure 9 **The optimal equilibrium z^* and the corresponding $\underline{b}(z^*)$ when** $B_0 = 10,370$

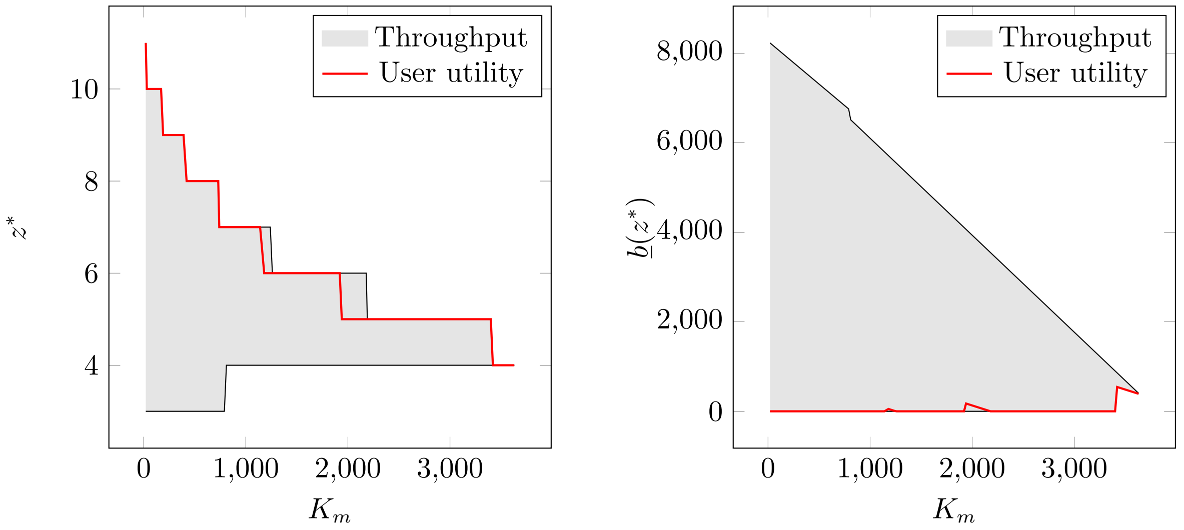

Figure 10 **The optimal equilibrium z^* and the corresponding $\underline{b}(z^*)$ when** $B_0 = 5,185$

or payment systems, e.g., secured data sharing, supply chain logistics monitoring, smart contracts, etc., and with multiple cryptocurrencies.

References

Antonopoulos AM (2014) *Mastering Bitcoin: unlocking digital cryptocurrencies* (" O'Reilly Media, Inc.").

Arnosti N, Weinberg SM (2018) Bitcoin: A natural oligopoly. *arXiv preprint arXiv:1811.08572* .

Babich V, Hilary G (2019) Distributed ledgers and operations: What operations management researchers should know about blockchain technology. *Manufacturing & Service Operations Management* .

Bagaria V, Kannan S, Tse D, Fanti G, Viswanath P (2018) Deconstructing the blockchain to approach physical limits. *arXiv preprint arXiv:1810.08092* .

Basu S, Easley D, O'Hara M, Sirer E (2019) Towards a functional fee market for cryptocurrencies. *Available at SSRN 3318327* .

Budish E (2018) The economic limits of bitcoin and the blockchain. Technical report, National Bureau of Economic Research.

Cong LW, He Z, Li J (2019) Decentralized mining in centralized pools. Technical report, National Bureau of Economic Research.

Cui Y, Hu M, Liu J (2018) Values of traceability in supply chains. *Available at SSRN 3291661* .

Easley D, O'Hara M, Basu S (2019) From mining to markets: The evolution of bitcoin transaction fees. *Journal of Financial Economics* .

Feldman P, Micali S (1988) Optimal algorithms for byzantine agreement. *Proceedings of the twentieth annual ACM symposium on Theory of computing*, 148–161 (ACM).

Garay J, Kiayias A, Leonardos N (2015) The bitcoin backbone protocol: Analysis and applications. *Advances in Cryptology - EUROCRYPT*, 281–310 (Berlin, Heidelberg: Springer), URL https://eprint.iacr.org/2014/765.pdf.

Gilad Y, Hemo R, Micali S, Vlachos G, Zeldovich N (2017) Algorand: Scaling byzantine agreements for cryptocurrencies. *Proceedings of the 26th Symposium on Operating Systems Principles*, 51–68 (ACM).

Hassin R (1995) Decentralized regulation of a queue. *Management Science* 41(1):163–173.

Hassin R (2016) *Rational queueing* (Chapman and Hall/CRC).

Huberman G, Leshno JD, Moallemi C (2021) Monopoly without a Monopolist: An Economic Analysis of the Bitcoin Payment System. *The Review of Economic Studies* ISSN 0034-6527, URL http://dx.doi.org/10.1093/restud/rdab014.

Kleinrock L (1967) Optimum bribing for queue position. *Operations Research* 15(2):304–318.

Kroll JA, Davey IC, Felten EW (2013) The economics of bitcoin mining, or bitcoin in the presence of adversaries. *Proceedings of WEIS*, volume 2013, 11.

Lavi R, Sattath O, Zohar A (2019) Redesigning bitcoin's fee market. *The World Wide Web Conference*, 2950–2956 (ACM).

Li C, Li P, Zhou D, Xu W, Long F, Yao A (2018) Scaling nakamoto consensus to thousands of transactions per second. *arXiv preprint arXiv:1805.03870* .

Lui FT (1985) An equilibrium queuing model of bribery. *Journal of political economy* 93(4):760–781.

Nakamoto S (2008) Bitcoin: A peer-to-peer electronic cash system https://bitcoin.org/bitcoin.pdf.

Pagnotta E (2018) Bitcoin as decentralized money: prices, mining, and network security. *Mining, and Network Security (July 12, 2018)* .

Pass R, Seeman L, Shelat A (2017) Analysis of the blockchain protocol in asynchronous networks. *Annual International Conference on the Theory and Applications of Cryptographic Techniques*, 643–673 (Springer).

Popov S (2016) The tangle. *cit. on* 131.

Prat J, Walter B (2018) An equilibrium model of the market for bitcoin mining .

Watson GN (1929) Theorems stated by ramanujan (v): Approximations connected with ex. *Proceedings of the London Mathematical Society* 2(1):293–308.

Wood G (2014) Ethereum: A secure decentralised generalised transaction ledger. *Ethereum project yellow paper* `https://ethereum.github.io/yellowpaper/paper.pdf`.

Yao ACC (2018) An incentive analysis of some bitcoin fee design. *arXiv preprint arXiv:1811.02351* .

Electronic Companion

Proof of Proposition 1 By (1), we can express the queueing latency as a function of θ as $W_q(\theta) = \frac{1}{\mu[1-(1+K)\theta^K + K\theta^{K+1}]}$. Taking the derivate of W_q yields that

$$\frac{dW_q(\theta)}{d\tilde{\lambda}} = W_q'(\theta)\frac{d\theta}{d\tilde{\lambda}} = \frac{K(K+1)}{\mu^2}\frac{(1-\theta)^3\,\theta^{K-1}}{[1-(1+K)\theta^K + K\theta^{K+1}]^3}$$

and θ is increasing in $\tilde{\lambda}$, W_q is increasing in $\tilde{\lambda}$ and it suffices to show that $\frac{(1-\theta)^3\theta^{K-1}}{\eta^3(\theta)}$, where $\eta(\theta) = 1-(1+K)\theta^K + K\theta^{K+1}$, is increasing in θ. Since

$$\frac{d}{d\theta}\left(\frac{(1-\theta)^3\theta^{K-1}}{\eta^3(\theta)}\right) = \frac{(1-\theta)^2\theta^{K-2}}{\eta^4(\theta)}[(K-1-(K+2)\theta)\eta(\theta) - 3\eta'(\theta)(1-\theta)\theta] \triangleq \frac{(1-\theta)^2\theta^{K-2}}{\eta^4(\theta)}h(\theta),$$

and $h(\theta) > 0$ when $K \le 3$, it suffices to show that $h(\theta) > 0$ for $\theta \in (0,1)$ and hence $h'(\theta) < 0$ given that $h(1) = 0$ for $K \ge 4$. We show this by establishing that $h'(\theta)$ has a unique global maximum $\theta = 1$ in $(0,1]$ at $h'(1) = 0$. Taking the derivatives, we obtain:

$$\begin{aligned} h'(\theta) =& -(K+2) + K(K+1)(2K+1)\theta^{K-1} + (K+1)(-4K^2-4K+2)\theta^K + K(K+2)(2K+1)\theta^{K+1},\\ h''(\theta) =& K(K+1)\theta^{K-2}[(K-1)(2K+1) + (-4K^2-4K+2)\theta + (K+2)(2K+1)\theta^2]. \end{aligned}$$

It can be easily shown that the term in "[ ]" in $h''(\theta)$ is quadratic with exactly two roots $\theta_1 < \theta_2$ in $(0,1)$. Thus, $h'(\theta)$ must achieve its global maxima at either θ_1 or 1. Since θ_1 is a root of $h''(\theta) = 0$, it satisfies $(K-1)(2K+1) + (-4K^2-4K+2)\theta_1 = -(K+2)(2K+1)\theta_1^2$ and $h'(\theta_1)$ can be reduced to

$$h'(\theta_1) = -(K+2) + 2K(2K+1)\theta_1^{K-1} - (4K^2+4K-2)\theta_1^K,$$

which is bounded from above by $\left\{\frac{4K+2}{K+2}\left[\frac{(2K+1)(K-1)}{2K^2+2K-1}\right]^{K-1} - 1\right\}(K+2)$. Applying $\ln(1-x) < -x - \frac{x^2}{2}$, we have:

$$\begin{aligned} &\frac{d}{dK}\ln\left[\frac{4K+2}{K+2}\left(\frac{(2K+1)(K-1)}{2K^2+2K-1}\right)^{K-1}\right]\\ =&\frac{6K^3+18K^2+9K+3+(K+2)(2K+1)(2K^2+2K-1)\ln(1-\frac{3K}{2K^2+2K-1})}{(K+2)(2K+1)(2K^2+2K-1)}\\ <&\frac{6K^3+18K^2+9K+3+(K+2)(2K+1)(-3K-\frac{9K^2}{2K^2+2K-1})}{(K+2)(2K+1)(2K^2+2K-1)}\\ =&\frac{-3(4K^4+11K^3+3K^2-K+1)}{(K+2)(2K+1)(2K^2+2K-1)^2} < 0 \end{aligned}$$

for $K \ge 1$. Since $\frac{4K+2}{K+2}(\frac{(2K+1)(K-1)}{2K^2+2K-1})^{K-1}|_{K=4} < 1$, $h'(\theta) < 0$ $\theta \in [0,1]$ for $K \ge 4$. □

Proof of Proposition 2 We first claim that $G^*(b)$ must be continuous for $b > \underline{b}$ for a given p^*. Suppose that $G^*(b+) > G^*(b-)$ at some b. Then, for ϵ sufficiently small, the cost difference for bidding at b and $b+\epsilon$ is $b + c(W(b-\epsilon|(p^*\Lambda, G^*), z)) - (b+\epsilon) - c(W(b+\epsilon|(p^*\Lambda, G^*), z)) > 0$. Thus, bidding at $b+\epsilon$ is preferred to bidding at b, and hence $G^*(\cdot)$ must be continuous.

Second, if $\underline{b}$ is the lowest bid allowed, the lowest bid must be $\underline{b}$ as it would otherwise cost users more to bid the lowest bid without lowering the queueing latency otherwise. □

Proof for Theorem 1 By Proposition 2, the support of the equilibrium fee distribution $G^*(\cdot)$ includes $\underline{b}$ and $G^*(\cdot)$ is continuous. Thus, (3) follows as the users' cost is the same for any bid b in the support, i.e., $\underline{b} + c\left(W_q(p^*\Lambda) + \frac{z}{\mu}\right) = b + c\left(W_q(p^*\Lambda(1 - G^*(b))) + \frac{z}{\mu}\right)$. Since the equilibrium joining probability $p^* \leq 1$, $p^* = 1$ if the users' utility $R - \underline{b} - c\left(W_q(\Lambda) + \frac{z}{\mu}\right) \geq 0$. Otherwise, p^* is given by $c(W_q(p^*\Lambda) + z/\mu) = R - \underline{b}$ and users' utility is 0 in equilibrium. Thus, we have (2).

Since the highest possible bid is the smallest solution to $\bar{G}^*(b) = 0$ or $\underline{b} + c\left(W_q(p^*\Lambda) + \frac{z}{\mu}\right) - c\left(\frac{z+1}{\mu}\right)$, (6) holds as

$$\begin{aligned}
\Phi^*(z) &= p^*\Lambda\underline{b} + \int_{\underline{b}}^{\underline{b}+c\left(W_q(p^*\Lambda)+\frac{z}{\mu}\right)-c(\frac{z+1}{\mu})} p^*\Lambda\bar{G}^*(b)db \\
&= p^*\Lambda\underline{b} + \int_{c\left(\frac{1+z}{\mu}\right)}^{c\left(W_q(p^*\Lambda)+\frac{z}{\mu}\right)} W_q^{-1}\left(c^{-1}(s) - \frac{z}{\mu}\right) ds \\
&= p^*\Lambda\underline{b} + \int_{1/\mu}^{W_q(p^*\Lambda)} W_q^{-1}(t)dc\left(t + \frac{z}{\mu}\right) \\
&= p^*\Lambda\underline{b} + \int_0^{p^*\Lambda} \tilde{\lambda}dc\left(W_q(\tilde{\lambda}) + \frac{z}{\mu}\right) \qquad \text{(EC.1)} \\
&= p^*\Lambda\underline{b} + p^*\Lambda c\left(W_q(p^*\Lambda) + \frac{z}{\mu}\right) - \int_0^{p^*\Lambda} c\left(W_q(\tilde{\lambda}) + \frac{z}{\mu}\right) d\tilde{\lambda} \\
&= p^*\Lambda \min\left\{R, \underline{b} + c\left(W_q(\Lambda) + \frac{z}{\mu}\right)\right\} - \int_0^{p^*\Lambda} c\left(W_q(\tilde{\lambda}) + \frac{z}{\mu}\right) d\tilde{\lambda}
\end{aligned}$$

and the expected utility of the users are given by (4). □

Proof for Proposition 3 $p^*(z)$ is decreasing in z and $G^*(b|z)$ is strictly increasing convex in b as $W_q(\cdot)$ and $c(\cdot)$ are both strictly increasing and convex, which imply that $W_q^{-1}(\cdot)$ and $c^{-1}(\cdot)$ are decreasing concave. Thus, $G^*(b|z) = 1 - \frac{W_q^{-1}\left(c^{-1}(R-b) - \frac{z}{\mu}\right)}{W_q^{-1}(c^{-1}(R-\underline{b}) - \frac{z}{\mu})}$ is increasing in z for $p^* < 1$ and $G^*(b|z)$ is a constant otherwise. □

Proof for Proposition 4 We first establish the log-concavity of $\Phi^*(z)$ for piece-wise linear $c(\cdot)$ functions. That is, for $0 = s_0 < s_1 < \cdots$, $k_1 < k_2 < \cdots$ and $w \in [s_{i-1}, s_i]$,

$$c(w) = d_0 + \sum_{j=0}^{i-1} k_j(s_j - s_{j-1}) + k_i(w - s_{i-1}). \tag{EC.2}$$

Suppose that $W_q(0) + \frac{z}{\mu} \in [s_{m-1}, s_m)$ and $W_q(p^*(z)\Lambda) + \frac{z}{\mu} \in [s_{n-1}, s_n)$. By (EC.1),

$$\begin{aligned}\Phi^*(z) &= \underline{b}p^*(z)\Lambda + \int_0^{p^*(z)\Lambda} \tilde{\lambda} dc\left(W_q(\tilde{\lambda}) + \frac{z}{\mu}\right) \\ &= \underline{b}p^*(z)\Lambda + \sum_{j=m}^{n-1}(k_{j+1} - k_j)\int_{s_j - \frac{z}{\mu}}^{W_q(p^*(z)\Lambda)} W_q^{-1}(\tilde{\lambda})d\tilde{\lambda} + k_m \int_0^{W_q\left(p^*(z)\Lambda\right)} W_q^{-1}(\tilde{\lambda})d\tilde{\lambda}\end{aligned}$$

and is differentiable even if $W_q(0) + \frac{z}{\mu} = s_{m-1}$ as

$$\lim_{\epsilon \downarrow 0} \frac{\Phi^*(z+\epsilon) - \Phi^*(z)}{\epsilon} - \lim_{\epsilon \downarrow 0} \frac{\Phi^*(z) - \Phi^*(z-\epsilon)}{\epsilon} = \frac{-(k_m - k_{m-1})W_q^{-1}\left(s_{m-1} - \frac{z}{\mu}\right)}{\mu} = 0.$$

Since

$$\begin{aligned}\frac{d\ln[\Phi^*(z)]}{dz} = \frac{\Phi^{*\prime}(z)}{\Phi^*(z)} &= \frac{-\underline{b}}{\mu W_q'(p^*(z)\Lambda)\Phi^*(z)} + \frac{-k_m p^*(z)\Lambda}{\mu\Phi^*(z)} \\ &\quad + \sum_{j=m}^{n-1}(k_{j+1} - k_j)\frac{W_q^{-1}\left(s_j - \frac{z}{\mu}\right) - W_q^{-1}\left(c^{-1}(R - \underline{b}) - \frac{z}{\mu}\right)}{\mu\Phi^*(z)} \le 0\end{aligned}$$

by applying $p^{*\prime}(z) = -\frac{1}{\Lambda\mu W_q'(p^*(z)\Lambda)}$ from (2), $\Phi^*(z)$ decreases in z. Furthermore, both the first term and the summands in the third term are all decreasing in z, by the concavity of $W_q^{-1}(\cdot)$. Note that $\frac{\Phi^*(z)}{p^*(z)\Lambda}$ is the expected fee paid by a user who joins the system and $G^*(\cdot|z)$ is the fee distribution in equilibrium. Since $G^*(\cdot|z)$ is stochastically decreasing in z, the second term is also decreasing in z. Thus, $\ln[\Phi^*(z)]$ is concave and, by the Weierstrass' approximation, remains concave for general increasing convex $c(\cdot)$ functions. □

Proof for Lemma 1 By Watson (1929) and Stirling's formula,

$$\frac{1}{2} \le \frac{1}{2} + \frac{n^n e^{-n}}{2n!} \le \sum_{k=0}^{z} \frac{z^k e^{-z}}{k!} \le \frac{1}{2} + \frac{2n^n e^{-n}}{3n!} \le \frac{1}{2} + \frac{2}{3\sqrt{2\pi z}}.$$

Since

$$0 < \sum_{k=z+1}^{\infty} \frac{(z\beta)^k}{k!} \le \sum_{k=z+1}^{\infty} \frac{(z\beta)^{z+1}}{(z+1)!}\left(\frac{z\beta}{z+2}\right)^{k-z-1} = \frac{(z\beta)^{z+1}}{(z+1)!}\frac{1}{1 - \frac{z\beta}{z+2}} \le \frac{1}{1-\beta}\frac{1}{\sqrt{2\pi z}}\beta^z e^{z(1-2\beta)},$$

we are able to obtain our bounds. □

Proof for Lemma 2 Since $\bar{\gamma}\left(\beta, \bar{z}(\beta,\delta)\right) = \underline{\gamma}(\beta, \underline{z}(\beta,\delta)) = \delta$,

$$\left[1 + \frac{\frac{4}{3} + \frac{2}{1-\beta}}{\sqrt{2\pi\bar{z}(\beta,\delta)}}\right]\left[\beta e^{(1-\beta)}\right]^{\bar{z}(\beta,\delta) - \underline{z}(\beta,\delta)} = 1.$$

Since $0 < \beta e^{(1-\beta)} < 1$ and $\bar{z}(\beta,\delta)$ is decreasing in δ for $0 \le \beta < 1$, $\bar{z}(\beta,\delta) - \underline{z}(\beta,\delta)$ is increasing in δ. □

Proof for Proposition 5 When $p^*(z) = 1$, $\underline{\gamma}\left(\frac{A}{\Phi^*(z)}, z\right)$ is decreasing. Thus, it suffices to show that the log of the function is quasi-convex when $p^*(z) < 1$. Letting

$$\frac{d}{dz}\left[\ln\left(\underline{\gamma}\left(\frac{A}{\Phi^*(z)}, z\right)\right)\right] = 0, \tag{EC.3}$$

we obtain

$$\left[\ln\left(\Phi^*(z)\right)\right]' = 1 + \frac{\ln\left(\frac{A}{\Phi^*(z)}\right)}{1 - \frac{A}{\Phi^*(z)}}. \tag{EC.4}$$

The left hand side is decreasing in z by Proposition 4 and the right hand side is increasing in z. Therefore, (EC.3) has at most one solution and the function is quasi-convex. □

Proof for Proposition 6 Due to the quasi-convexity of $\underline{\gamma}\left(\frac{A}{\Phi^*(z)}, z\right)$, the sequence is monotonic and hence either converges to an equilibrium or diverges to infinity. The initial conditions determine whether the sequence increases or decreases. See Figure 2 for a graphical illustration. □

Proof for Lemma 3 It suffices to show that

$$\Phi^*\left(z\middle|\frac{\eta}{K_m}, K_m, \left[R - c\left(W_q\left(\Lambda\middle|\frac{\eta}{K_m}, K_m\right) + \frac{zK_m}{\eta}\right)\right]^+\right) \ge \Phi^*(z|\mu, K, \underline{b}) \ge \Phi^*\left(z\middle|\frac{\eta}{K_m}, K_m, 0\right)$$

which implies that there is a desired $\underline{b}(z)$ such that $\left(z, \frac{\eta}{K_m}, K_m, \underline{b}(z)\right)$ is feasible, and

$$\lambda^*(z|\mu, K, \underline{b}) \le \lambda^*\left(z\middle|\frac{\eta}{K_m}, K_m, \left[R - c\left(W_q\left(\Lambda\middle|\frac{\eta}{K_m}, K_m\right) + \frac{zK_m}{\eta}\right)\right]^+\right) = \lambda^*\left(z\middle|\frac{\eta}{K_m}, K_m, 0\right).$$

By (2), λ^* is maximized when $\underline{b} = \left[R - c\left(W_q(\Lambda|\mu, K) + \frac{z}{\mu}\right)\right]^+$ for given (μ, K, z) and

$$\begin{aligned}
\lambda^*(z|\mu, K, \underline{b}) &\leq \lambda^*\left(z\middle|\mu, K, \left[R - c\left(W_q(\Lambda|\mu, K) + \frac{z}{\mu}\right)\right]^+\right) = \min\left\{W_q^{-1}\left(c^{-1}(R) - \frac{z}{\mu}\middle|\mu, K\right), \Lambda\right\} \\
&\leq \lambda^*\left(z\middle|\frac{\eta}{K}, K, \left[R - c\left(W_q\left(\Lambda\middle|\frac{\eta}{K}, K\right) + \frac{zK}{\eta}\right)\right]^+\right) \\
&\leq \lambda^*\left(z\middle|\frac{\eta}{K_m}, K_m, \left[R - c\left(W_q(\Lambda|\mu, K) + \frac{z}{\mu}\right)\right]^+\right) \qquad \text{(EC.5)}
\end{aligned}$$

where the last two inequalities follow as $W_q(\lambda|\mu, K)$ is decreasing in μ for a given (λ, K), and, by Lemma EC.1 below, $W_q\left(\lambda\middle|\frac{\eta}{K}, K\right)$ is increasing in K for a given λ. Note that

$$\frac{\partial \Phi^*(z|\mu, K, \underline{b})}{\partial \underline{b}} = \begin{cases} \Lambda > 0, & \text{if } \underline{b} < \left[R - c\left(W_q(\Lambda|\mu, K) + \frac{z}{\mu}\right)\right]^+, \\ \underline{b}\frac{\partial \lambda^*(z|\mu, K, \underline{b})}{\partial \underline{b}} < 0, & \text{if } \underline{b} > \left[R - c\left(W_q(\Lambda|\mu, K) + \frac{z}{\mu}\right)\right]^+ \end{cases}$$

and

$$\Phi^*\left(z\middle|\mu, K, \left[R - c\left(W_q(\Lambda|\mu, K) + \frac{z}{\mu}\right)\right]^+\right) = \int_0^{\lambda^*\left(z\middle|\mu, K, \left[R - c\left(W_q(\Lambda|\mu, K) + \frac{z}{\mu}\right)\right]^+\right)} \left[R - c\left(W_q(\tilde{\lambda}|\mu, K)\right)\right] d\tilde{\lambda}$$

increases in μ as both the upper limit and the integrand are non-negative and increasing in μ. Thus,

$$\begin{aligned}
\Phi^*(z|\mu, K, \underline{b}) &\leq \Phi^*\left(z\middle|\mu, K, \left[R - c\left(W_q(\Lambda|\mu, K) + \frac{z}{\mu}\right)\right]^+\right) \\
&\leq \Phi^*\left(z\middle|\frac{\eta}{K}, K, \left[R - c\left(W_q\left(\Lambda\middle|\frac{\eta}{K}, K\right) + \frac{zK}{\eta}\right)\right]^+\right) \\
&\leq \Phi^*\left(z\middle|\frac{\eta}{K_m}, K_m, \left[R - c\left(W_q\left(\Lambda\middle|\frac{\eta}{K_m}, K_m\right) + \frac{zK_m}{\eta}\right)\right]^+\right).
\end{aligned}$$

The last inequality follows a similar argument as the previous one and Lemma EC.1.

It remains to show that $\Phi^*(z|\mu, K, \underline{b}) \geq \Phi^*\left(z\middle|\frac{\eta}{K_m}, K_m, 0\right)$. By the optimality of $(z, \mu, K, \underline{b})$, equality holds for (EC.5), implying that either $(\mu, K, \underline{b}) = \left(\frac{\eta}{K_m}, K_m, \left[R - c\left(W_q\left(\Lambda\middle|\frac{\eta}{K_m}, K_m\right) + \frac{zK_m}{\eta}\right)\right]^+\right)$ or $\lambda^*(z|\mu, K, \underline{b}) = \Lambda$. For the former, the result holds trivially. Otherwise, it follows from (6) that $(\tilde{\mu}, \tilde{K}, \tilde{\underline{b}}) = (\frac{\eta}{K_m}, K_m, 0)$ minimizes $\Phi^*(z|\tilde{\mu}, \tilde{K}, \tilde{\underline{b}})$ when $\lambda^*(z|\tilde{\mu}, \tilde{K}, \tilde{\underline{b}}) = \Lambda$. Hence $\Phi^*(z|\frac{\eta}{K_m}, K_m, 0) \leq \Phi^*(z|\mu, K, \underline{b})$. □

Lemma EC.1. *For a given λ, $W_q\left(\lambda\middle|\frac{\eta}{K}, K\right)$ is increasing in K.*

Proof of Lemma EC.1 Letting $\theta \in (0,1)$ be the unique solution to $\frac{\theta-\theta^{K+1}}{1-\theta} = K\frac{\lambda}{\eta}$, we have

$$W_q\left(\lambda\middle|\frac{\eta}{K}, K\right) = \frac{K}{\eta[1-(1+K)\theta^K + K\theta^{K+1}]} = \frac{\theta}{(1-\theta)\left[\lambda(1+K) - (\eta+\lambda K)\theta\right]}. \tag{EC.6}$$

It is obvious that $W_q(\lambda|\eta,1) < W_q\left(\lambda\middle|\frac{\eta}{2}, 2\right)$. Thus, it suffices to show that $\frac{d}{dK}W_q\left(\lambda\middle|\frac{\eta}{K}, K\right) > 0$ for $K \in [2,\infty)$, which is equivalent to

$$\frac{(\eta+2\lambda K+\lambda)\,\theta}{\lambda(1+K)-(\eta+\lambda K)\,\theta^2} > \frac{-\eta\theta^{K+1}\ln(\theta)}{\lambda K(1-\theta)} + 1 - \frac{1}{K} \tag{EC.7}$$

by applying

$$\frac{d\theta}{dK} = \frac{\theta\left[\lambda(1-\theta)+\eta\theta^{K+1}\ln(\theta)\right]}{K\left[\lambda(1+K)-(\eta+\lambda K)\,\theta\right]}.$$

Since $1+\frac{\lambda}{\eta}K - \frac{\lambda K}{\theta\eta} = \theta^K \in \left(0, \frac{\lambda}{\eta}\right)$, $\theta \in \left(\frac{\lambda K}{\eta+\lambda K}, \frac{\lambda K}{\eta-\lambda+\lambda K}\right)$. Therefore,

$$\frac{(\eta+2\lambda K+\lambda)\,\theta}{\lambda(1+K)-(\eta+\lambda K)\,\theta^2} > \frac{K\,(\eta+2\lambda K+\lambda)}{(1+K)\eta+\lambda K}.$$

Furthermore,

$$\theta^K < \left(\frac{\lambda K}{\eta-\lambda+\lambda K}\right)^K \le \frac{2\lambda^2 K}{\left[\lambda^2+\eta^2\right]K-(\eta-\lambda)^2}$$

and $-\frac{\ln(\theta)}{1-\theta} \le \frac{1}{\theta}$, implying that for $K \ge 2$,

$$\frac{-\eta\theta^{K+1}\ln(\theta)}{\lambda K(1-\theta)} + 1 - \frac{1}{K} < \frac{2\lambda}{\left[\lambda^2+\eta^2\right]K-(\eta-\lambda)^2} - \frac{1}{K} + 1 \le \frac{K\,(\eta+2\lambda K+\lambda)}{(1+K)\eta+\lambda K}$$

Thus, (EC.7) and hence, the lemma hold. □

Proof for Lemma 4 The second statement follows by Proposition 5 with $\underline{b} = 0$. For ease of notation, we denote $b_1(z) = \left[R - c\left(W_q\left(\Lambda\middle|\frac{\eta}{K_m}, K_m\right) + \frac{zK_m}{\eta}\right)\right]^+$.

If $R - c\left(W_q\left(\Lambda\middle|\frac{\eta}{K_m}, K_m\right) + \frac{K_m}{\eta}\right) < 0$, then $b_1(z) = 0$ for all $z \ge 1$, and $\underline{\gamma}\left(\frac{A}{\Phi^*\left(z\middle|\frac{\eta}{K_m}, K_m, b_1(z)\right)}, z\right)$ is quasi-convex.

If $R - c\left(W_q\left(\Lambda\middle|\frac{\eta}{K_m}, K_m\right) + \frac{K_m}{\eta}\right) \ge 0$, let z_0 be the smallest such that $R - c\left(W_q\left(\Lambda\middle|\frac{\eta}{K_m}, K_m\right) + \frac{z_0 K_m}{\eta}\right) \le 0$. Then,

$$\begin{aligned}&\Phi^*\left(z\middle|\frac{\eta}{K_m}, K_m, b_1(z)\right)\\ &= \begin{cases} \int_0^{\Lambda}\left[R - c\left(W_q\left(\lambda\middle|\frac{\eta}{K_m}, K_m\right) + \frac{zK_m}{\eta}\right)\right]d\lambda, & \text{if } z \le z_0,\\ \int_0^{W_q^{-1}\left(c^{-1}(R) - \frac{zK_m}{\eta}\middle|\frac{\eta}{K_m}, K_m\right)}\left[R - c\left(W_q\left(\lambda\middle|\frac{\eta}{K_m}, K_m\right) + \frac{zK_m}{\eta}\right)\right]d\lambda, & \text{if } z > z_0.\end{cases}\end{aligned}$$

Note that $\ln\left(\int_0^{\Lambda}\left[R - c\left(W_q\left(\lambda\middle|\frac{\eta}{K_m}, K_m\right) + \frac{zK_m}{\eta}\right)\right]d\lambda\right)$ is decreasing concave in z as $c\left(W_q\left(\lambda\middle|\frac{\eta}{K_m}, K_m\right) + \frac{zK_m}{\eta}\right)$ is increasing convex in z. Following a similar argument as in the proof of Proposition 5, we have that $\underline{\gamma}\left(\frac{A}{\int_0^\Lambda\left[R-c\left(W_q(\lambda\left|\frac{\eta}{K_m},K_m)+\frac{zK_m}{\eta}\right)\right]d\lambda\right.},z\right)$ and $\underline{\gamma}\left(\frac{A}{\int_0^{W_q^{-1}\left(c^{-1}(R)-\frac{zK_m}{\eta}\left|\frac{\eta}{K_m},K_m\right.\right)}\left[R-c\left(W_q\left(\lambda\left|\frac{\eta}{K_m},K_m\right.\right)+\frac{zK_m}{\eta}\right)\right]d\lambda},z\right)$ are quasi-convex for $z\geq 0$.

When $z\leq z_0$, $W_q^{-1}\left(c^{-1}(R)-\frac{zK_m}{\eta}\middle|\frac{\eta}{K_m},K_m\right)\geq\Lambda$ and hence,

$$\begin{aligned}&\underline{\gamma}\left(\frac{A}{\int_0^\Lambda\left[R-c\left(W_q\left(\lambda\middle|\frac{\eta}{K_m},K_m\right)+\frac{zK_m}{\eta}\right)\right]d\lambda},z\right)\\ &\geq\underline{\gamma}\left(\frac{A}{\int_0^{W_q^{-1}\left(c^{-1}(R)-\frac{zK_m}{\eta}\left|\frac{\eta}{K_m},K_m\right.\right)}\left[R-c\left(W_q\left(\lambda\middle|\frac{\eta}{K_m},K_m\right)+\frac{zK_m}{\eta}\right)\right]d\lambda},z\right).\end{aligned}$$

Therefore, $\underline{\gamma}\left(\frac{A}{\Phi^*\left(z\left|\frac{\eta}{K_m},K_m,b_1(z)\right.\right)},z\right)$ is quasi-convex. □

Proof of Lemma 5 The feasibility of $(z,\frac{\eta}{K_m},K_m,\underline{b}(z))$ follows from Lemma 3 if $(z,\mu,K,\underline{b})$ is feasible. Here, the users' utility can be reformulated as

$$U^*(z|\mu,K,\underline{b})=\Lambda R-\Phi^*(z|\mu,K,\underline{b})-\int_0^\Lambda c\left(W_q(\lambda|\mu,K)+\frac{z}{\mu}\right)d\lambda.$$

Since $\Phi^*(z|\mu,K,\underline{b})=\Phi^*\left(z\middle|\frac{\eta}{K_m},K_m,\underline{b}(z)\right)$ and $W_q(\lambda|\mu,K)+\frac{z}{\mu}\geq W_q\left(\lambda\middle|\frac{\eta}{K_m},K_m\right)+\frac{zK_m}{\eta}$ with equality holds only when $(\mu,K)=\left(\frac{\eta}{K_m},K_m\right)$, $U^*(z|\mu,K,\underline{b})\leq U^*\left(z\middle|\frac{\eta}{K_m},K_m,\underline{b}(z)\right)$. □

Proof of Lemma 6 Here, we prove the lemma for differentiable $c(\cdot)$. Since any convex function can be approximated by a sequence of differentiable convex functions, the result follows for general $c(\cdot)$. It suffices to show that

$$\frac{dU^*(\Phi^*)}{d\Phi^*}=-1+\frac{\ln(2\delta)}{A\frac{\eta}{K_m}}\frac{\left(\frac{A}{\Phi^*}\right)^2-\frac{A}{\Phi^*}}{\left[1-\frac{A}{\Phi^*}+\ln\left(\frac{A}{\Phi^*}\right)\right]^2}\cdot\int_0^\Lambda c'\left(W_q\left(\lambda\middle|\frac{\eta}{K_m},1\right)+\frac{\ln(2\delta)}{\frac{\eta}{K_m}}\frac{1}{1-\frac{A}{\Phi^*}+\ln(\frac{A}{\Phi^*})}\right)d\lambda=0$$

has a unique solution. Since $\frac{\left(\frac{A}{\Phi^*}\right)^2-\frac{A}{\Phi^*}}{\left[1-\frac{A}{\Phi^*}+\ln\left(\frac{A}{\Phi^*}\right)\right]^2}$ is increasing in $\Phi^*>A$ with $\lim_{\frac{A}{\Phi^*}\downarrow 0}\frac{\left(\frac{A}{\Phi^*}\right)^2-\frac{A}{\Phi^*}}{\left[1-\frac{A}{\Phi^*}+\ln\left(\frac{A}{\Phi^*}\right)\right]^2}=0$ and $\lim_{\frac{A}{\Phi^*}\uparrow 1}\frac{\left(\frac{A}{\Phi^*}\right)^2-\frac{A}{\Phi^*}}{\left[1-\frac{A}{\Phi^*}+\ln\left(\frac{A}{\Phi^*}\right)\right]^2}=-\infty$, $\frac{\ln(2\delta)}{A\frac{\eta}{K_m}}\frac{\left(\frac{A}{\Phi^*}\right)^2-\frac{A}{\Phi^*}}{\left[1-\frac{A}{\Phi^*}+\ln\left(\frac{A}{\Phi^*}\right)\right]^2}\geq 0$ and decreases in Φ^*. Noting that the integration is also non-negative and decreasing in Φ^* by the convexity of $c(\cdot)$, we have $\frac{dU^*(\Phi^*)}{d\Phi^*}$ is decreasing in Φ^*. Thus, $\lim_{\Phi^*\downarrow A}\frac{dU^*(\Phi^*)}{d\Phi^*}=+\infty$ and $\lim_{\Phi^*\uparrow+\infty}\frac{dU^*(\Phi^*)}{d\Phi^*}=-1$ guarantee a unique solution $\hat{\Phi}^*$. Since $U^*\left(\Phi^*\left(z_3\middle|\frac{\eta}{K_m},1,0\right)\right)=0$, $\frac{dU^*(\Phi^*)}{d\Phi^*}|_{\Phi^*=\Phi^*\left(z_3\left|\frac{\eta}{K_m},1,0\right.\right)}\leq 0$ and $\hat{\Phi}^*=\Phi^*\left(z^*(\hat{\Phi}^*)\middle|\frac{\eta}{K_m},1,0\right)\leq\Phi^*\left(z_3\middle|\frac{\eta}{K_m},1,0\right)$, implying that $z^*(\hat{\Phi}^*)\geq z_3$. □

Proof of Theorem 3 Since $\underline{\gamma}\left(\frac{A}{\Phi^*(z^*)}, z^*\right) < \underline{\gamma}\left(\frac{A}{\Phi^*(z^*)}, z^*-1\right)$ and both functions are quasi-convex, $\underline{\gamma}\left(\frac{A}{\Phi^*(z^*)}, z^*-1\right) = \delta$ has at most two roots $z_1' \leq z_2'$ such that $z_1^* < z_1' \leq z_2' \leq z_2^*$ and all the integers in $[z_1^*, z_1')$ and $(z_2', z_2^*]$ are equilibria. Furthermore, $\underline{\gamma}\left(\frac{A}{\Phi^*(\lceil z_1^*\rceil)}, \lceil z_1^*\rceil - 1\right) \geq \underline{\gamma}\left(\frac{A}{\Phi^*(\lceil z_1^*\rceil - 1)}, \lceil z_1^*\rceil - 1\right) > \delta$ implies $z_1' > \lceil z_1^*\rceil$. □

Proof of Proposition 10 The constraints of the reduced optimization problem analogous to (15)-(17) can be written as

$$\underline{\gamma}\left(\frac{A}{B_0 + \Phi^*\left(z \middle| \frac{\eta}{K_m}, K_m, \left[R - c\left(W_q\left(\Lambda \middle| \frac{\eta}{K_m}, K_m\right) + \frac{zK_m}{\eta}\right)\right]^+\right)}\right) \leq \delta, \tag{EC.8}$$

$$\underline{\gamma}\left(B_0 + \frac{A}{\Phi^*\left(z \middle| \frac{\eta}{K_m}, K_m, 0\right)}, z-1\right) > \delta. \tag{EC.9}$$

Due to the monotonicity of the objective function, the first statement follows from the same reasoning as that of Proposition 7. Note that when $\lambda^*\left(z \middle| \frac{\eta}{K_m}, K_m, 0\right) = \Lambda$, the left side of (EC.8) is quasi-convex while the left side of (EC.9) is decreasing in z. Thus, the second statement follows. □

Proof of Proposition 12 Following a similar argument as that provided in the proof of Theorem 1, we can show that G^* is continuous for any given p^*. Next, we show that b increases in C. Suppose that $c_1 < c_2$ but $b_1 > b_2$. As a result, it is more costly for users with c_1 to bid at b_2 than at b_1, i.e.,

$$b_1 + c_1 W_q\left((1 - G^*(b_1)p^*\Lambda)\right) \leq b_2 + c_1 W_q((1 - G^*(b_2)p^*\Lambda))$$

or

$$W_q\left((1 - G^*(b_2))p^*\Lambda\right) - W_q((1 - G^*(b_2))p^*\Lambda) \geq \frac{b_1 - b_2}{c_1}.$$

Hence, it is more costly for users with c_2 to bid at b_2 than at b_1 as

$$[b_2 + c_2 W_q((1 - G^*(b_2))p^*\Lambda)] - [b_1 + c_2 W_q((1 - G^*(b_1))p^*\Lambda)] \geq b_2 - b_1 + \frac{c_2}{c_1}(b_1 - b_2) > 0,$$

which contradicts with the definition of an equilibrium.

The monotonicity of b depending on C implies that users with a waiting cost $C(qp^*)$ bid at $b(q)$ in equilibrium, i.e., $b(q)$ is a minimizer of the total cost $b + C(qp^*) W_q((1 - G^*(b))p^*\Lambda)$. By the first-order optimality condition, we have:

$$\frac{db(q)}{dq} = C(qp^*) W_q'((1-q)p^*\Lambda).$$

Solving the above differential equation with the boundary condition $b(0) = \underline{b}$, we obtain the desired result for $b(q)$. The total cost of bidding at $b(q)$ is given by

$$\begin{aligned}
& b(q) + C(qp^*)\left(W_q((1-q)p^*\Lambda) + \frac{z}{\mu}\right) \\
&= \underline{b} + \int_{(1-q)p^*}^{p^*} C(p^* - p)\, dW_q(p\Lambda) + C(qp^*)\left(W_q((1-q)p^*\Lambda) + \frac{z}{\mu}\right) \\
&= b(0) + C(0)W_q(p^*\Lambda) + \int_{(1-q)p^*}^{p^*} W_q(p\Lambda) dC(p^* - p) + C(qp^*)\frac{z}{\mu},
\end{aligned}$$

and is increasing in q. Thus, p^* is the largest such that $b(1) + C(p^*)\left(\frac{1+z}{\mu}\right) \le R$. The expression of Φ^* follows immediately. □

Proof of Proposition 13 Again we can show that G^* is continuous for any given p^*. We first consider that $c(\cdot)$ is strictly convex and show that b increases in Z^*. Suppose that $z_1 < z_2$ but $b_1 > b_2$. Then, it is more costly for users with z_1 to bid at b_2 than at b_1, i.e.,

$$b_1 + c\left(W_q((1 - G^*(b_1)p^*\Lambda)) + \frac{z_1}{\mu}\right) \le b_2 + c\left(W_q((1 - G^*(b_2)p^*\Lambda)) + \frac{z_1}{\mu}\right)$$

or

$$c\left(W_q((1 - G^*(b_2)p^*\Lambda)) + \frac{z_1}{\mu}\right) - c\left(W_q((1 - G^*(b_1)p^*\Lambda)) + \frac{z_1}{\mu}\right) \ge b_1 - b_2.$$

Since $c(\cdot)$ is strictly convex,

$$\begin{aligned}
&\left[b_2 + c\left(W_q((1 - G^*(b_2))p^*\Lambda) + \frac{z_2}{\mu}\right)\right] - \left[b_1 + c\left(W_q((1 - G^*(b_1))p^*\Lambda) + \frac{z_2}{\mu}\right)\right] \\
&> b_2 - b_1 + (b_1 - b_2) = 0,
\end{aligned}$$

i.e., it is more costly for users with z_2 to bid at b_2 than at b_1, which contradicts with the definition of an equilibrium.

The monotonicity of b depending on Z^* implies that users with a confirmation latency $\frac{\ln\left[2\Delta(1-qp^*)\right]}{1-\frac{A}{\Phi}+\ln\left(\frac{A}{\Phi}\right)}$ bid at $b(q)$ in equilibrium, i.e., $b(q)$ is a minimizer of the total cost $b + c\left(W_q((1-G^*(b))p^*\Lambda)+\frac{\ln\left[2\Delta(1-qp^*)\right]}{\mu\left[1-\frac{A}{\Phi}+\ln\left(\frac{A}{\Phi}\right)\right]}\right)$. By the first-order optimality condition, we have:

$$\frac{db(q)}{dq}=c'\left(W_q\left((1-q)\,p^*\Lambda\right)+\frac{\ln\left[2\Delta(1-qp^*)\right]}{\mu\left[1-\frac{A}{\Phi}+\ln\left(\frac{A}{\Phi}\right)\right]}\right)W_q'((1-q)p^*\Lambda).$$

Solving the above differential equation with the boundary condition $b(0)=\underline{b}$, we obtain the desired result for $b(q)$. The total cost of bidding at $b(q)$ is given by

$$\begin{aligned}
&b(q)+c\left(W_q((1-q)p^*\Lambda)+\frac{\ln\left[2\Delta(1-qp^*)\right]}{\mu\left[1-\frac{A}{\Phi}+\ln\left(\frac{A}{\Phi}\right)\right]}\right)\\
&=\underline{b}+\int_{(1-q)p^*}^{p^*}c'\left(W_q(p\Lambda)+\frac{\ln\left[2\Delta(1-p^*+p)\right]}{\mu\left[1-\frac{A}{\Phi}+\ln\left(\frac{A}{\Phi}\right)\right]}\right)dW_q(p\Lambda)+c\left(W_q((1-q)p^*\Lambda)+\frac{Z^*(qp^*)}{\mu}\right)\\
&=b(0)+c\left(W_q(p^*\Lambda)+\frac{\ln\left[2\Delta(1)\right]}{\mu\left[1-\frac{A}{\Phi}+\ln\left(\frac{A}{\Phi}\right)\right]}\right)\\
&\quad+\int_{(1-q)p^*}^{p^*}c'\left(W_q(p\Lambda)+\frac{\ln\left[2\Delta(1-p^*+p)\right]}{\mu\left[1-\frac{A}{\Phi}+\ln\left(\frac{A}{\Phi}\right)\right]}\right)d\left(\frac{\ln\left[2\Delta(1-p^*+p)\right]}{-\mu\left[1-\frac{A}{\Phi}+\ln\left(\frac{A}{\Phi}\right)\right]}\right),
\end{aligned}$$

and is increasing in q. Thus, p^* is the largest such that $b(1)+c\left(\frac{1}{\mu}+\frac{\ln\left[2\Delta(1-p^*)\right]}{\mu\left[1-\frac{A}{\Phi}+\ln\left(\frac{A}{\Phi}\right)\right]}\right)\leq R$. The expression of Φ^* follows immediately.

When $c(\cdot)$ is not strictly convex, we can use a sequence of strictly convex functions $[1+(1+c(x))^n]^{\frac{1}{n}}$ to approximate $c(x)$, since $\lim_{n\to\infty}[1+(1+c(x))^n]^{\frac{1}{n}}=c(x)$. Thus, the results still hold when $c(\cdot)$ is not strictly convex. □